Meccanica

Vibrational analysis for surge precursor definition in gas turbines

--Manuscript Draft--

Manuscript Number:	MECC-D-18-00742R1
Full Title:	Vibrational analysis for surge precursor definition in gas turbines
Article Type:	Original papers
Section/Category:	Machines
Keywords:	Vibrations, surge precursors, monitoring, gas turbines
Corresponding Author:	federico Reggio, M.D. Universita degli Studi di Genova Genoa, ITALY
Corresponding Author Secondary Information:	
Corresponding Author's Institution:	Universita degli Studi di Genova
Corresponding Author's Secondary Institution:	
First Author:	federico Reggio, M.D.
First Author Secondary Information:	
Order of Authors:	federico Reggio, M.D.
	Mario Luigi Ferrari
	Paolo Silvestri
	Aristide Fausto Massardo
Order of Authors Secondary Information:	
Funding Information:	
Abstract:	Compressor behaviour analysis in critical working conditions, such as incipient surge, represents a significant aspect in the turbomachinery research field. Turbines connected with large-size volumes present critical issues related to surge prevention especially during transient operations. Investigations based on acoustic and vibrational measurements appear to provide an interesting diagnostic and predictive solution by adopting suitable quantifiers calculated from microphone and accelerometer signals. For this scope a wide experimental activity has been conducted on a T100 microturbine connected with different volume sizes. A machine dynamical characterisation has been useful for better interpretation of signals during its transient to the surge. Hence, different possible methods of incipient surge identification have been developed through the use of different signal processing techniques in time, frequency and angle domain. These results will be useful for control system development to prevent compressor failures.
Response to Reviewers:	Reviewer #1 •The paper should deal with the identification of surge precursors (as stated from the author) nevertheless it only reports the techniques already known in literature. We have tried to better explain the innovative aspects of our work including the following sentence in the introduction: “After a preliminary machine vibration response analysis, based on standard techniques, most of this paper is devoted to the development of different surge precursors for application in advanced gas turbine cycles. Considering that no surge prevention techniques are implemented in commercial machines, this innovation is very important for systems based on the coupling of microturbines with large-volume-size components.” Thank you.

	•The motivation is clearly stated, nevertheless the objective is not focused. The discussion appears to be not well balanced between the innovative work and the system identification and characterization of the test rig in use. We have removed Figure 3, Figure 5 and Figure 6 and their related text from section 4 (“Preliminary machine vibratory response analysis”) to make the paper balanced and more related to its main focus. Thank you. •From the perspective of the reviewer there is a misalignment between the study proposed in this paper and the journal publication target. Thanks for the clarification/suggestion. However, we think that Meccanica journal covers a wide range of topics in the mechanical engineering field. For sure, it is difficult to find another paper exactly about our subject, but as example we found some manuscripts that regard topics similar to what we presented, such as: - “Surge instability in a distributed parameter radial compression system”, Volume 30, Issue 1, February 1995, Pages 37-52. - “Structural monitoring of “Himera” viaduct by low-cost MEMS sensors: characterization and preliminary results”, Volume 52, Issue 13, 1 October 2017, Pages 3221-3236. - "A three-degree-of-freedom model for vortex-induced vibrations of turbine blades", Volume 51, Issue 11, 1 November 2016, Pages 2607-2628. - “Vibration-based diagnostics of gearboxes under variable speed and load conditions”, Volume 51, Issue 12, 1 December 2016, Pages 3227-3239. - “Multivariable optimal control of an industrial nonlinear boiler–turbine unit”, Volume 51, Issue 4, 1 April 2016, Pages 859-875. •The layout of the plots should be revised in order to keep the layout uniform throughout the reading. The layout of the plots has been revised. Now graphs of figures 9, 11, 13, 21 and 29 have the same format. Thank you. • Several sentences must be rewritten in order to guarantee a better comprehension. We are sorry if some sentences were too long or not fluent. We have revised our manuscript on the basis of a mother tongue reviewer. Thank you. Reviewer #2: •From a general point of view, the first part on dynamic characterization for resonance detection is somewhere too detailed and could be easily softened to let the reader to more quickly arrive to the main issue of the paper - the surge precursors. We have removed Figure 3, Figure 5 and Figure 6 and their related text from section 4 (“Preliminary machine vibratory response analysis”) to make the paper balanced and more related to its main focus. Thank you. •A concern that should be addressed by the Authors is also how they define the surge event and the surge pulse. In other words, in the text a sound criterion on how they define the surge is not clearly shown. In the reviewer opinion, a preliminary statement on this issue should be added to the paper. In section 4 “Preliminary machine vibratory response analysis” we tried to clarify how we define the surge event and the surge pulse. For this reason, the following text has been added: “The goal of this work is to find surge precursors useful to prevent instability, which when it starts can be identified by a rapid system response energy increment and the presence of some low frequency contents related to the surge flow and pressure cycles. As surge pulse, the rapid pressure variation that is related to the strong flow

	reversal was considered: at the beginning of a surge cycle the pressure at the impeller exit and diffuser drops rapidly whereas the pressure in the impeller inlet increases, causing an impulsive dynamic forcing that stresses the blades, the rotor and the structure of the machine [29]". •Another concern is related to the application. The Authors should comment on the generality of their findings since they are applying their investigation to a very particular machine which has distinctive peculiarity with respect to other compressors (such as, for instance, the high rotational speed). Thank you for your interest regarding our result application, in the conclusion we have added: "The results presented above are relative to a microturbine because advanced cycles and innovative plant layouts are (usually conceived for distributed generation) related to this machine size. However, the techniques presented in this paper to find surge precursors could also be, in general, applicable for large-size machines." We hope to have met your doubts and questions and we thank you for your careful reading and interest shown in our work. Kind Regards, F. Reggio, M.L. Ferrari, P. Silvestri, A.F. Massardo

Vibrational analysis for surge precursor definition in gas turbines

F. Reggio, M.L. Ferrari, P. Silvestri, A.F. Massardo
Thermochemical Power Group (TPG)
University of Genoa, Italy

Contact author: F. Reggio (federico.reggio@edu.unige.it)
Telephone no. +39 3396528711

Abstract

Compressor behaviour analysis in critical working conditions, such as incipient surge, represents a significant aspect in the turbomachinery research field. Turbines connected with large-size volumes present critical issues related to surge prevention especially during transient operations.
Investigations based on acoustic and vibrational measurements appear to provide an interesting diagnostic and predictive solution by adopting suitable quantifiers calculated from microphone and accelerometer signals. For this scope a wide experimental activity has been conducted on a T100 microturbine connected with different volume sizes. A machine dynamical characterisation has been useful for better interpretation of signals during its transient to the surge. Hence, different possible methods of incipient surge identification have been developed through the use of different signal processing techniques in time, frequency and angle domain. These results will be useful for control system development to prevent compressor failures.

Keywords

Vibrations, surge precursors, monitoring, gas turbines.

1. Introduction

The use of gas turbine technology in advanced cycles and innovative plant layouts (e.g. humid cycles, hybrid systems and integration with renewable energy sources) implies the need for a greater development of the monitoring system to extend the operating range of these machines, their performance and reliability to allow integration with the other plant components [1]. Key aspects

are the prediction and prevention of stall and dangerous surge phenomena [2][3][4] which produce damage to the compressor [5][6]. Commercial turbines are not equipped with surge prevention systems since their standard operations are controlled to be in the safe zone, as managed by the manufacturer's control system. However, plants including additional components, which increase the volume size located between the compressor outlet and the combustor inlet [7], operate with significant compressor surge risk [8]. Especially during transient operations, when operational point can reach the stability line due to the increase in response modification. A simple machine shutdown, in case of surge event, could be critical if plants include components which cannot tolerate fast property variations (e.g. high-temperature heat exchangers or fuel cells) [9].

Recently a new research approach based on surge precursors seems to be promising and complementary to other techniques based on compressor performance studies [11][12][13][14][14]. It is based on the analysis of machine vibro-acoustic signals which are also interesting because they come from non-intrusive standard sensors.

Some authors have tried to find stall or surge precursors from compressor and turbocharger compressor vibro-acoustic signals [15]. Researchers from the National Technical University of Athens [16] tested a turbocharger compressor with microphones observing an increase in low frequency energy content below rotational frequency. So, they proposed using the RMS value of the sub-synchronous part of the spectrum as a parameter to distinguish compressor operating regimes. Significant studies have been developed in [17][18]. During two experimental works, they tested a six-axial and one-centrifugal-stage compressor. In the first work they found sub-synchronous activity in the spectrum map of the accelerometers mounted in correspondence with the axial stages when the throttle valve was nearest to closed position. In detail, some peaks appear at about 30-40% of the rotational speed. This sub-synchronous activity could be associated with the onset of stall since stall and surge are related to each other and the former often precedes the latter. In a second experimental work, cyclostationary analysis was presented on the basis of acceleration and microphone signals: they identified stall considering some sub-synchronous modulation frequencies which, in case of small discharge volume, changed frequency before they disappeared at surge conditions with its corresponding modulation frequency. This change is probably due to (a) new stall cell/s generated (new blades that stall) and seems to be a surge precursor.

In this article some analysis results of vibro-acoustic signals from a T100 Turbec microturbine (with a centrifugal compressor) will be presented. The aim of the research is related to possible surge precursors from non-intrusive sensors such as accelerometers and microphones using analysis in the time, frequency and angle domain. These new, different analytical methods have been applied to the same set of data to obtain sufficiently independent surge precursors also useful synergistically to

enhance knowledge in the diagnostic system. Data could be acquired thanks to the availability of an experimental facility [19] based on a T100 turbine developed by the Thermochemical Power Group (TPG) at the University of Genoa. It was possible to analyse sound and vibrational signals not from a single independent component (compressor) installed in a dedicated line, but from an entire small size turbomachine inserted in a plant to distribute generation with three different volume configurations. So, the compressor does not work in stand-alone mode, but its operation and rotational speed are linked to the behaviour of the other components. In detail, machine operational regime and so vibro-acoustic signals contain all plant vibration and sound contribution: thus, they are more realistic of real compressor use in the plant.

After a preliminary machine vibration response analysis, based on standard techniques, most of this paper is devoted to the development of different surge precursors for application in advanced gas turbine cycles. Considering that no surge prevention techniques are implemented in commercial machines, this innovation is very important for systems based on the coupling of microturbines with large-volume-size components.

2. The test rig

The TPG experimental test rig is composed of a modified microturbine (T100 machine: 100kW electrical power at 70,000rpm nominal rotation speed, 30% nominal efficiency thanks to a recuperated cycle) and external vessels placed between the recuperator outlet and the combustor inlet [8][20]. Although they were designed for the emulation of hybrid systems with a Solid Oxide Fuel Cell (SOFC)[7], these vessels can represent systems with large volume size connected to a gas turbine [8].

In this work, the vessels were used just as additional volume components, not only specifically for SOFC. Moreover, the vibrational analysis results reported in this paper were carried out for general advanced cycles based on gas turbines. To simulate different kinds of microturbine based plant, three different volume configurations were considered and tested: 4.1m^3, 2.3m^3 and 0.3m^3 (values of the external additional volume connected to the T100 microturbine). The 4.1m^3 configuration, obtained summing the entire modular vessel and the anodic side, is representative of an SOFC based hybrid system, the 2.3m^3, with three module pipes fewer, refers to a plant with a high temperature storage device and the 0.3m^3, resulting from a direct connection between recuperator and turbine, stands for a system with a small volume additional component (e.g. an additional heat exchanger).

Figure 1 shows the test rig layout: the plant has two main control valves VM and VO to manage the connection with vessels, a check valve located downstream of the compressor outlet and a bleed

on/off emergency valve to discharge part of the air flow. Three air/water heat exchangers located in the compressor inlet ducts (EX) are also used to control compressor inlet temperature.

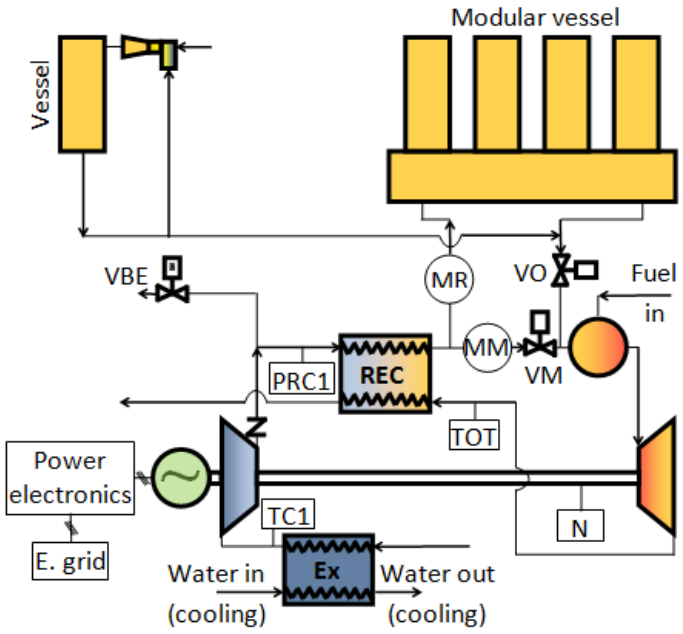

Fig.1 Test rig layout

Performance data are measured and acquired by the control software developed in LabVIEW™ which permits management of the plant from the control room and saves measures with 0.1s acquisition time step.

The original gas turbine control system guarantees safe turbine operation: it controls the fuel flow to make Turbine Outlet Temperature (TOT) constant at 918.15K and operates the machine start-up and shutdown phases.

Siemens Scadas mobile acquisition system was used to acquire vibro-acoustic measurement signals during the machine run-up, during the transient from a steady-state condition to the surge and during the successive run-down when the control system turn off the machine. The acquisition system can acquire 8 different signals simultaneously with a sampling frequency up to 204.8kHz. A tachometer signal was derived from the generator current frequency: so, it is synchronous and comparable with all the other signals from accelerometers and microphone. A tri-axial accelerometer and a mono-axial accelerometer (axial direction) were placed on the electric generator case close to the rotor ball bearing and the compressor inlet. These sensors have dynamic characteristics that allow frequency investigation up to 10kHz. To study the blade pass frequency, two micro accelerometers with resonance frequency higher than 55kHz (radial direction) and higher than 80kHz (axial direction) were also used. Finally, a pre-polarised Gras microphone with a dynamic response in the range between 2 and 50kHz was placed to acquire sound at the compressor inlet [21][22][20].

3. Experimental test and data acquisition

Data acquisition was carried out during several test days in which the T100, connected with one of the three additional volume configurations (0.3m^3, 2.3m^3, 4.1m^3), worked in grid-connected mode with the variable-speed control system which maintained the Turbine Outlet Temperature (TOT = 918.15K) constant.

The turbine was started-up to a production of 40kW electrical load (rotational speed at about 62,000rpm). This initial condition was selected considering the following purposes: significant off-design condition (usually these advanced systems need to be very flexible in terms of part-load operations), initial condition with a large margin from surge, avoidance of too low load values where the machine control system reduces the Turbine Outlet Temperature (TOT) set-point, and a feasible initial condition with the plant equipment (e.g. the VBE size).

After reaching this steady-state operative condition, surge phenomenon was generated progressively closing the VO valve (in 2.3m^3 and 4.1m^3 cases) or the VM valve (0.3m^3 case) placed in the air path between recuperator outlet and combustor inlet (increasing the pressure loss). These valves were closed by successive steps of 10% (5% close to the surge line) until the surge event in a range between 20-30% of valve opening. Vibro-acoustic acquisitions were started before every valve motion until the system reached a new steady-state condition. So, successive data sets containing signals from all sensors were collected. A sampling rate of 8,196Hz was chosen because it permits the signals to contain all significant frequencies: during the transient to the surge, rotational speed remained in the range between 62,000 and 65,000rpm (1,033-1,083Hz) [23][24]. This influenced the choice because sample frequency has to be much higher than double the rotational frequency [25] to permit the analysis of all sub-synchronous content (useful field to find surge precursors). A higher sampling rate (up to 200kHz) was adopted for a micro accelerometer aiming to study frequencies around the blade pass frequency (about 13kHz). As surge was reached, only a few cycles were acquired because the control system immediately switched-off the machine to limit damage risks. However, the turbine run down at low speed (between 9,000 and 20,000rpm) has a slower deceleration with a cleaner tachometer signal than the run up. So, acquisition of both ramps seems to be useful for the machine dynamic identification.

4. Preliminary machine vibratory response analysis

To improve surge precursor research, some considerations about stable and safe machine vibrational behaviour could be carried out to better distinguish surge contributions. Vibro-acoustic signals were acquired during machine start-up and shutdown operations at the beginning and at the

end of each surge test with the three volume configurations. Thus, run-up and run-down acquisitions were obtained collecting vibro-acoustic data during a large speed interval. Ramps were managed by T100 automatic control system which forces a specific motion law. The transient operations were not excessively fast allowing us to identify the dynamics of the system: each speed value corresponds to a machine operating regime in a safe condition from the surge. Vibration analysis in these safe conditions allows us to identify, for each microturbine speed, the frequency contents in the vibration signals and to associate them with their sources.

Figure 2 reports the waterfall representation of a time-frequency analysis of compressor axial vibration spectra evaluated in correspondence with the roll bearing at the generator during a run up between 12,000 and 70,000rpm. The horizontal, vertical and the inclined axes represent, respectively, the frequency, the vibration amplitude and the compressor rotational speed (spectra were calculated at regular speed intervals). For the vibration speed amplitude, integration was also performed to better underline vibration low frequency contents.

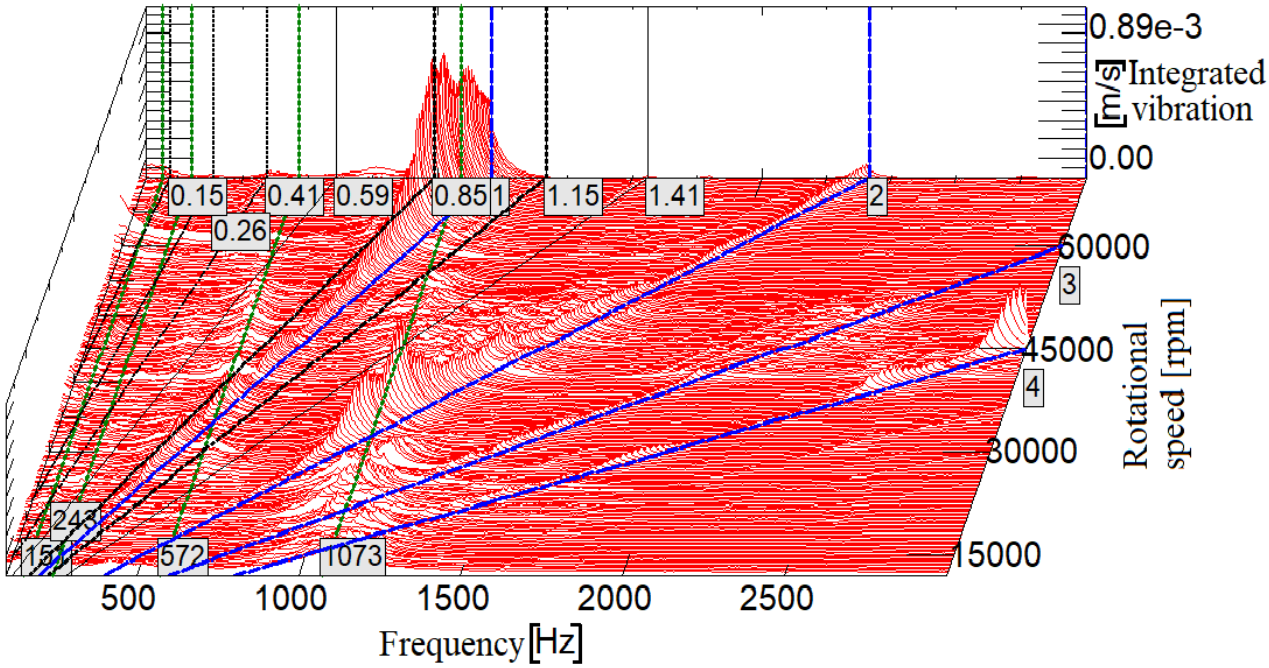

Fig.2 Microturbine run up: waterfall of integrated axial accelerometer signal at the generator bearing (volume 2.3m^3)

In the waterfall figure, sloping cursors were used to relate measured vibration frequencies to multiples of the microturbine shaft rotational frequency [25][26][27]. Some contents or orders change their frequency linearly with speed: those contents which have the same frequency as the rotational speed (1X) and the double (2X) seem due to the rotor imbalances in presence of non-linearity in the system, while the fourfold (4X) might be due to the two-polar-pair generator which magnetically solicits the rotor periodically. Other multiples might be referred to some bearing

typical operational frequencies (e.g. a component close to the 3X might be referred to rolling bearing ball spin frequency). Furthermore, in the waterfall, it is possible to note frequency contents probably related to a modulation phenomenon [28] of the sub-synchronous components on the 1X (see the cursor 0.82X and 1.15X) sidebands. It is interesting to note that all these contents found in the start-up waterfall become more relevant when they are coupled with possible structural resonance facilitating their identification. At the higher frequencies (not visible in figure) the blade pass frequency (BPF) 13X content must be mentioned, which presents two sidebands due to modulation phenomenon related to 1X.

A tachometer signal acquired together with the acoustic and vibrational measures allows us to plot the RMS amplitude trend of the single order frequency contents during speed ramps. In figure 3 the run up (A) and run down (B) of 1X order trends are shown in two different graphs: each graph includes 1X trends (coloured continuous lines) from different test days with the same 2.3m^3 volume configuration (in Figure 3 the black line refers to the 1X order trend in the Figure 2 waterfall). For the same type of ramp (run up/run down) 1X RMS amplitude curves are not significantly different from their mean values (red dotted line) which are therefore sufficiently representative of system dynamics (useful to identify its resonances). As in the waterfall diagrams, in the order plot an amplitude increase is shown when the first order is coupled with the system resonances (see black dotted cursors) during the ramp. Some peaks appear close and sometimes joined by the overlap of their widths due to damping. These couples of close peaks are probably rotor resonances corresponding to the same vibrational mode (about two different radial directions with different stiffness).

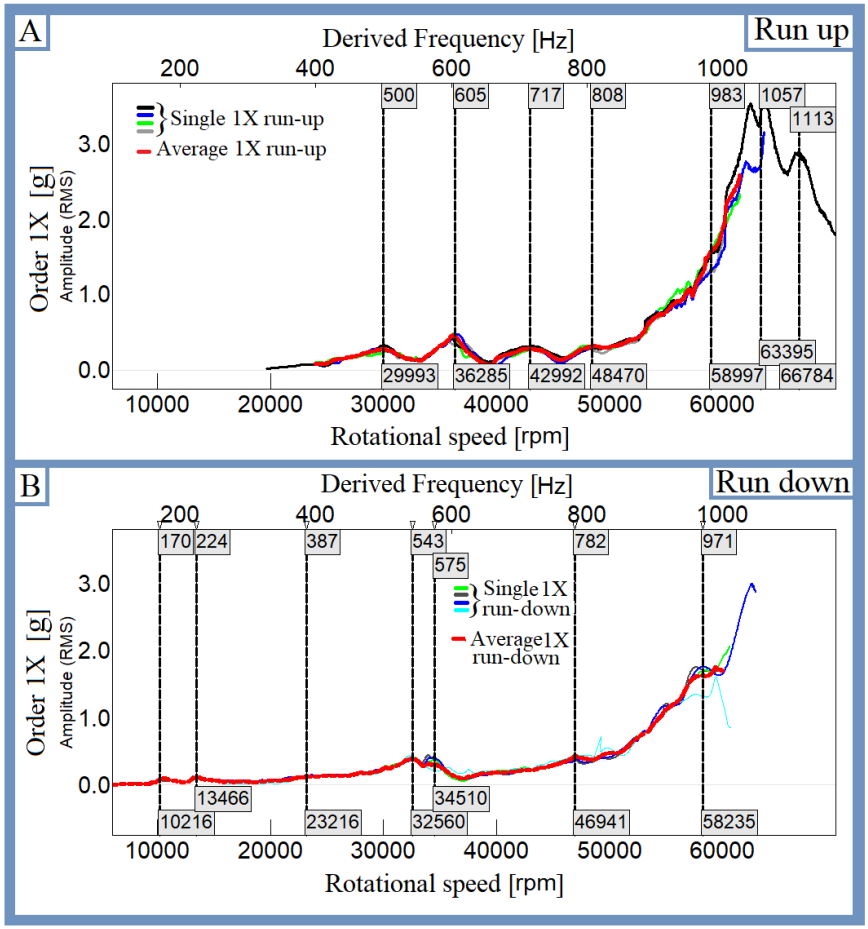

Fig.3 Run-up and run-down 1X trends with their means in function of speed and its correspondent converted frequency (volume 2.3m^3)

Some resonances are present in the range between 150 and 230Hz while another interesting range is between 470 and 620Hz. In this range the presence of a resonance is confirmed by the machine control system behaviour that (during the run up) increases the acceleration to rapidly pass it (Figure 5 higher acceleration after 35,000rpm). Other peaks are present between 700 and 800Hz and close to 950Hz. These last frequencies (probably less dangerous) have more energy because, during the ramp, the machine passed through their speed slowly (with a low acceleration). They are interesting because they were obtained close to the test machine rotational speed. Differences between run-up and run-down trends lead to slightly different resonance frequencies: this might be due to different speed ramps and angular acceleration levels which have a certain influence on the system dynamic vibratory response.

System resonances and dynamic response identification through 1X order is possible in the 0-1000Hz interval, which is the range corresponding to the explored machine rotational speed interval during a run up or a run down. Some significant superior orders (2X 4X), due to sources with higher frequency acceleration, pass resonances faster (so 2X and 4X have lower energy), but can reach

higher frequencies (double and quadruple compared to 1X). Their analysis seems to add 1,115Hz, 1,549Hz and 1,857Hz to the possible resonance frequencies previously found.

1X order and its multiple-trend analysis during speed ramps provide general useful information for characterisation of system dynamic behaviour and for the identification of its characteristic/critical frequencies. However, analysing different vibration orders, the possible system resonance frequencies are found at operative speed imposed by orders themselves: every mode cannot be excited at the same machine operative speed, but only at that speed corresponding to the mode's own frequency. This because the analysed order is due to a load/forcing synchronous with the speed (e.g. 1X order is due to rotor residual imbalance which forces the system with the same frequency of the machine rotation).

To test a further method of system dynamic behaviour analysis, at operative speed as close as possible to that at which we want to diagnose the incipient pumping phenomenon, auto-power spectrum was calculated in correspondence of a surge pulse.

The goal of this work is to find surge precursors useful to prevent instability, which when it starts can be identified by a rapid system response energy increment and the presence of some low frequency contents related to the surge flow and pressure cycles. As surge pulse, the rapid pressure variation that is related to the strong flow reversal was considered: at the beginning of a surge cycle the pressure at the impeller exit and diffuser drops rapidly whereas the pressure in the impeller inlet increases, causing an impulsive dynamic forcing that stresses the blades, the rotor and the structure of the machine [29].

This analysis was based on the following hypothesis: surge generated excitation, being of impulsive nature, has broadband characteristics with enough energy to excite the system at least in the whole field of sub-synchronous frequencies. So, system resonances can be obtained also when the system is subjected to the same external fluid-dynamic and mechanical actions (e.g. centrifugal field influences system rigidity) present in the operative incipient condition to be analysed.

Figure 4A shows accelerometer signal in axial direction during the compressor surge obtained by closing VO valve until 20% of its maximum opening (volume 4.1m^3). Coloured plots underline the 0.1s signal windows used to calculate auto-power spectrum: this limited windowing was chosen to obtain a sufficient frequency resolution avoiding the effects due to overlap of successive different pulses.

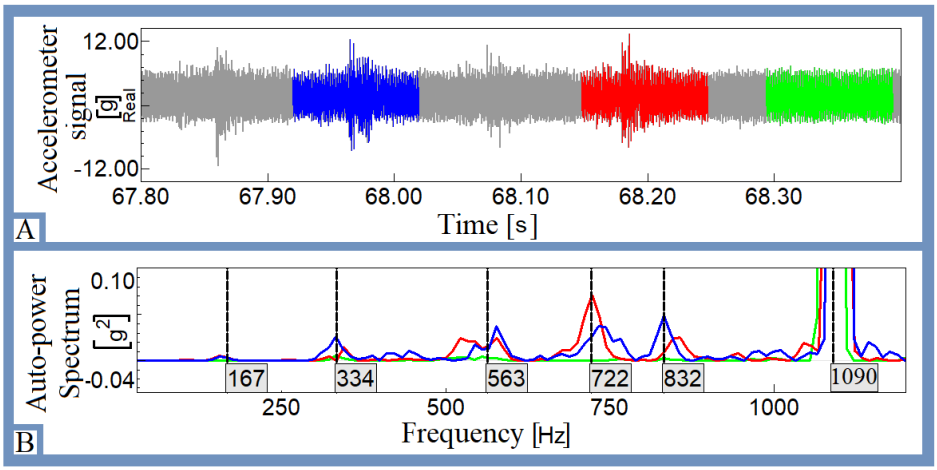

Fig.4A: accelerometer signal during surge with used 0.1s windows coloured
B: auto-power spectra calculated from the corresponding signal windows

In Fig. 4B the signal plot in function of the time spectra corresponding to the three windows are shown: all spectra have the highest peak in correspondence with the machine rotational frequency (1,090Hz), but blue and red spectra have some peaks of energy around 167Hz, 334Hz, 563Hz, 722Hz and 832Hz that are less visible in the signal spectrum without the pulse (green). This confirms the hypothesis that surge pulse can solicit broadband the machine which responds with its resonances.

Figure 5 shows the same spectra with some just mentioned contents (elliptical markers), but underlining presence of some peaks at the double frequencies of two resonances at about 523Hz and 576Hz. These peaks appear only in the spectra correspondent to a surge pulse when high energy is given to the system due to system non-linear behaviour (in its non-linear normal modes [30][31] it responds to the high energy given with more than one frequency content).

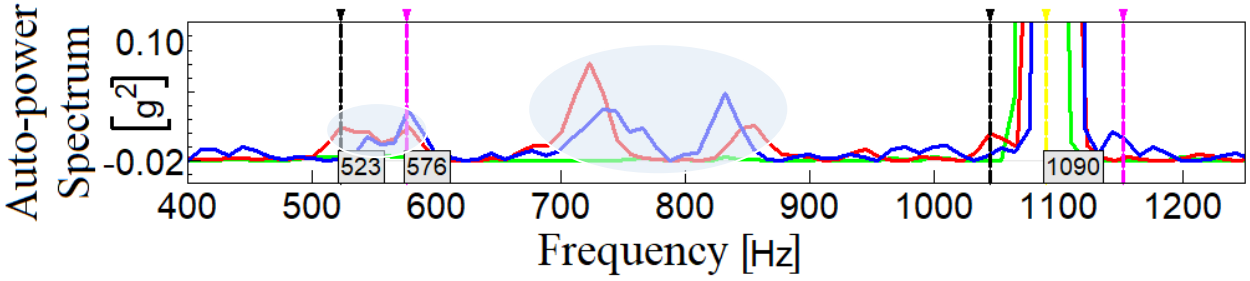

Fig.5 Auto-power spectra during surge: some peaks at the double frequency of some resonances

System vibratory contents, measured during surge pulses, provide useful indications to find surge premonitory contributes. They seem to be the natural frequencies of system operative condition and both surge phenomenon and surge incipience seem able to solicit them introducing broadband energy in the system. Consequently, if some of these components manifested themselves sufficiently in advance, they would be useful unstable-condition precursors helping to avoid surge.

Research on system characteristic frequencies was done for the three different plant-volume configurations finding comparable frequency values in all cases: measured vibrational response seems to be mainly conditioned by microturbine characteristics and to depend less on the structural dynamics of the plant line. Through the results of the run-up/down analysis and spectrum, during the surge it was possible to extract information about system dynamics and to find its operative characteristic frequencies, which seem to be the contents that have to be better taken into account in the monitoring phase to diagnose the incipience of the surge phenomenon.

Frequencies obtained during run up and run down, although found in operational conditions farther than those of the surge approach tests, are useful to validate those frequencies obtained during instability pulses. Table 1 shows all the frequencies found from the above-mentioned analysis, frequencies reported in the same row are considered related to the same critical condition.

Run-up frequencies [Hz]	Run-down frequencies [Hz]	Surge pulse frequencies [Hz]
(*)	170	167
(*)	224	(*)
(*)	(*)	334
(*)	387	(*)
500	543	523
605	575	576
717	(*)	722
808	782	832
983	971	(*)
1057	(*)	1,046
1,113	1,115	1,152
(*) Frequency not detectable in the corresponding method.		

Table.1 Comparison of critical excited frequencies extracted from different operational data

5. Spectral analysis during the transient to the surge.

Considering previous works from literature [16][17][18][15], it was possible to focus our attention on the analysis for the identification of surge precursors.

Surge condition for the three volume configurations ($0.3m^3$, $2.3m^3$ and $4.1m^3$) were generated through a transient in which the VM (in $0.3m^3$ case) or VO (in $2.3m^3$ and $4.1m^3$ cases) valve was closed step by step (step of 10-5%). So consecutive runs containing the signals from all sensors during each valve closure step were collected.

Inside the time interval of each run, ranges of 5s were chosen far enough from the valve motion and a few seconds (5s) before the surge for runs containing system response when it reaches instability. So, these signals are not influenced by the valve moving and represent an operating regime characterised by a given valve closure percentage and/or the surge incipience condition. These

intervals of 5s, being machine status representative, were used for most of the different signal analyses that will be presented in this paper.

Firstly, extracts were used to calculate an auto-power spectrum for each closure percentage (valve step) and to study the signal evolution to the surge. For this purpose, spectra were calculated as the average of 5 spectra obtained from a Hanning window [32] of 1s inside the 5s interval.

As shown in literature [16][17][18][15], sub-synchronous frequency ranges are interesting for the surge prediction because they do not include contents due to vibrational sources such as residual imbalance or other phenomena associated with the microturbine rotational speed and higher multiples. So, its energy (RMS value) is more sensitive to the approach of an incipient surge and increase progressively approaching it. Although all the accelerometer signal directions show an increase in RMS value, the most sensitive one is the axial direction, which coincides with the machine rotational axis and the mass flow inlet direction. As examples, in Figures 6 and 7 some auto-power spectra are shown for different valve openings from far to immediately before surge event for the 4.1m^3 volume configuration (see also figure 15 for the 2.3m^3 configuration).

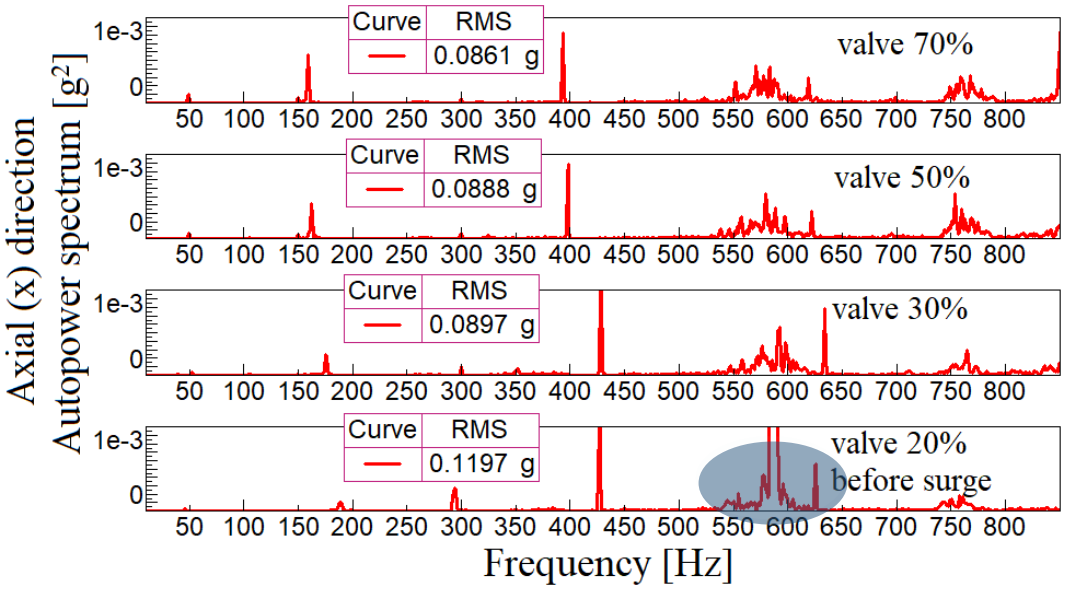

Fig.6 Sub-synchronous auto-power spectrum of accelerometer signal in axial direction for different values of valve opening and its RMS value (4.1m^3 volume)

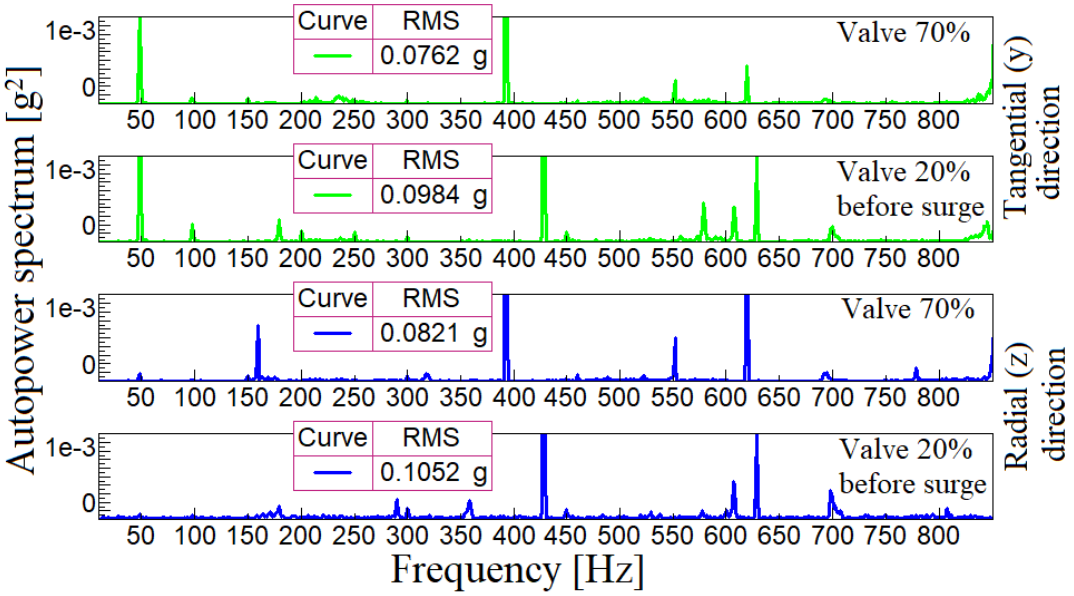

Fig.7 Sub-synchronous auto-power spectrum of accelerometer signal in tangential (Y) and radial (Z) directions for different values of valve opening and its RMS value (4.1m^3 volume)

In all volume configurations the surge incipience adds broadband noise in the sub-synchronous field increasing its RMS value progressively. In Figure 8, among the different volume configurations that with 2.3m^3 is more sensitive with a broad band energy increase before surge (see figure 16 for 2.3 m^3 configuration auto power spectra for some valve steps from far to near the surge). In all volume configurations, within the sub-synchronous field, an energy increase has been found in the band around 575 Hz approaching the surge (figure 6 elliptical marker), this seem due to the surge incipience broadband source that excites a just above found system resonance.

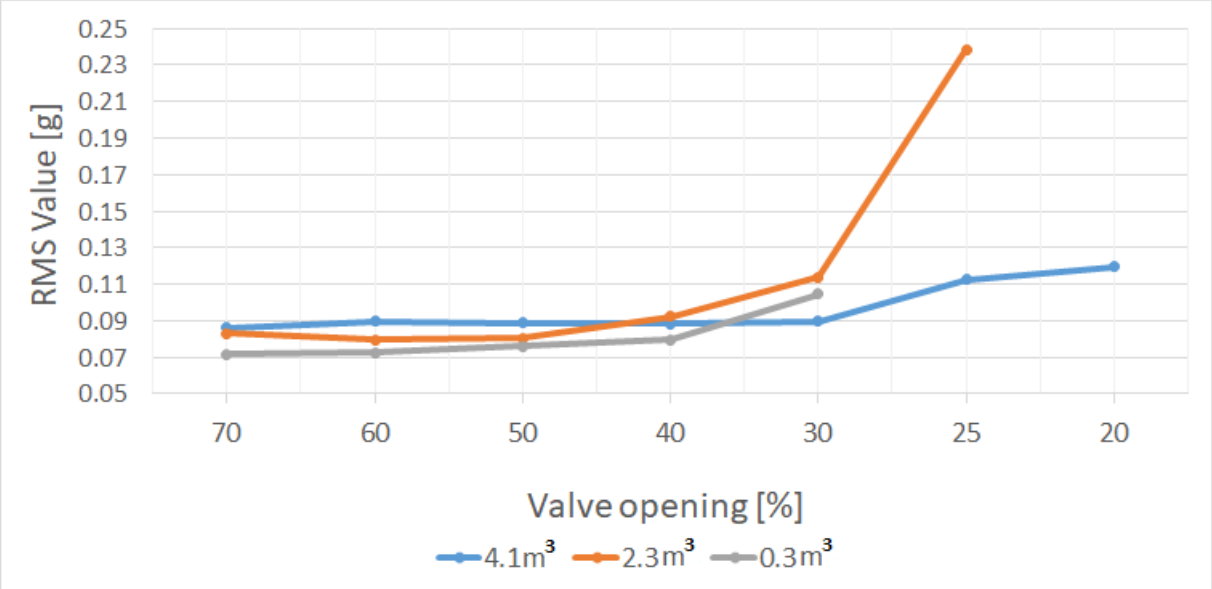

Fig.8 Axial accelerometer sub-synchronous RMS energy trends joining each value at different valve closure

Microphone signal spectrum in low frequency (0-80 Hz) presents higher energy (Fig.9), while the dynamics of the structure of the machine make accelerometer frequency content under 40 Hz less noticeable (Fig. 6 and 7). The very low frequencies (less than 19 Hz) have a high energy content, but do not follow a specific trend through the approaching surge. These contents can be related to the presence of cooling fans that introduce noise in the band 0-19 Hz and make the measured acoustic response not directly related to the microturbine compressor operating condition.

High energy and a more defined peak correspond to a component around 50Hz which almost disappears in the $0.3m^3$ volume configuration. Only for the $2.3m^3$ configuration does it progressively increase before surge. This component could be due to the resonance of a plant component, probably the air volume between the filter and compressor inlet inside the microturbine box. Between these two contents in a range from 19Hz to 37Hz (the range between faint dotted cursors in figure 9) there are one or more contents which increase before surge in all kinds of configurations: their trends are shown in figure 10.

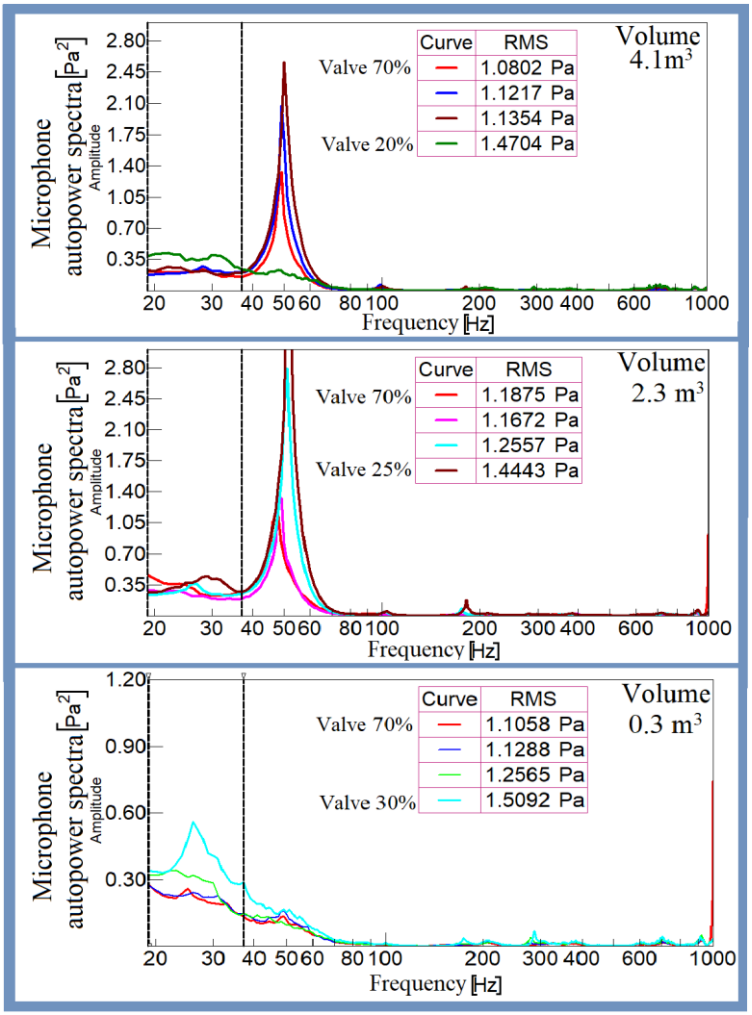

Fig.9 Microphone auto-power spectrum for different valve closures and their RMS energy value in the 19-37Hz band

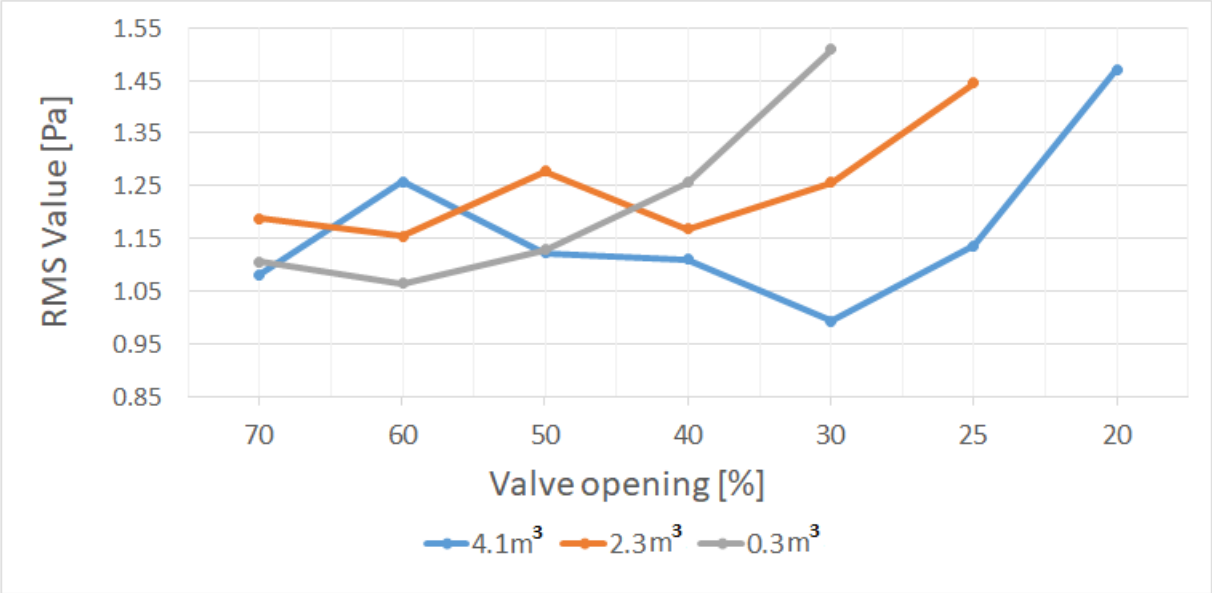

Fig.10 19 to 37Hz RMS energy trends for different volume configurations

This band is interesting because its energy is higher than the microphone sub-synchronous contents over 80Hz and increases before the surge event until it reaches an RMS value quite similar for all volumes (1.44-1.51Pa). So, it seems to be very useful as a surge precursor.

Although sub-synchronous contents over 80Hz of the microphone auto-power spectrum have less energy, it seems useful to consider the RMS energy of the entire band between 80 and 800Hz which has an increasing trend progressively towards the surge. Therefore, it can be another possible precursor.

As an example, Figure 11 shows the 80-800Hz microphone auto-power spectrum for different valve closure values from 70% opened to 20% in the plant configuration with 4.1m^3: it is possible to note the difference of energy between far (70%) from the instability (red spectrum) and near (20% the last 5s before surge) the surge (dark green spectrum). Figure 12 shows microphone 80-800Hz RMS trends for the three different-volume configurations.

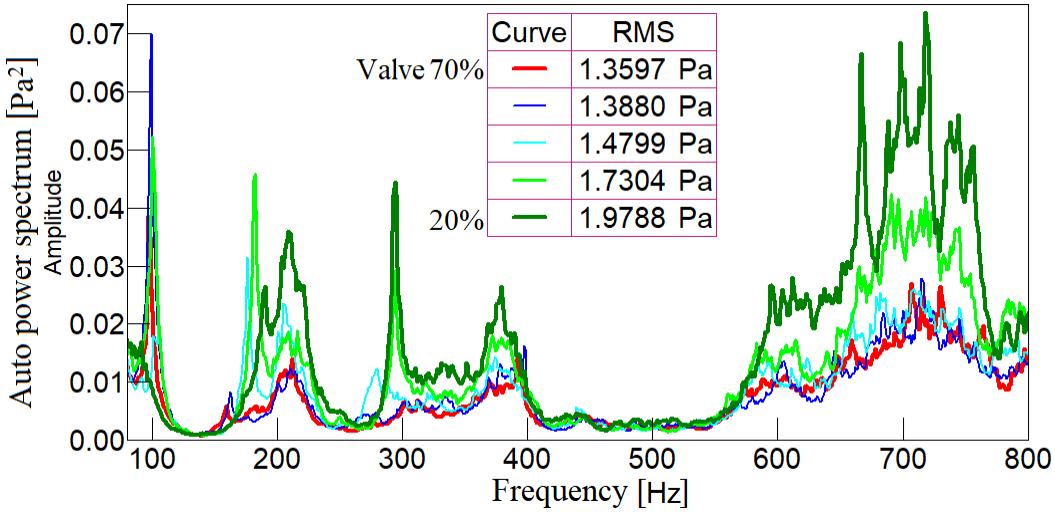

Fig.11 Microphone 80-800Hz sub-synchronous auto-power spectrum for 4.1m^3 plant configuration

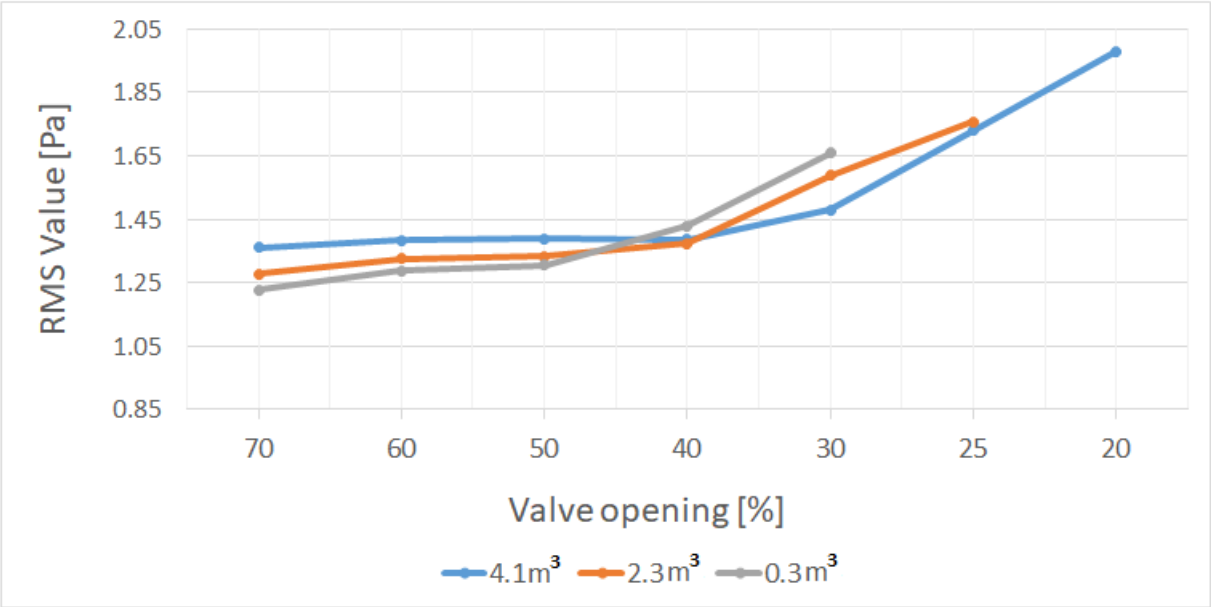

Fig.12 Sub-synchronous (80-800Hz) microphone RMS value presents energy increasing in all volume configurations

Having evaluated the RMS sub-synchronous value of different operational conditions and valve closures, it is necessary to check if the valve moving can affect this value. The consecutive signal runs, acquired during the transitory to the surge, can be concatenated to gain a unique signal also including vibrational response during valve closure. Sub-synchronous RMS energy value can be calculated in function of time during the valve transient to the surge. Figures 13 and 14 show that RMS value calculated during each valve step regime (Figure 13 in the table of each spectrum) are also present in the complete transient operations (green cursors in figure 14). So, RMS value appears to have a progressive trend without relevant abnormal discontinuity and peaks during valve movement: thus it seems to be more sensitive to compressor operating conditions than to the

moving of the delivery valve on the main mass flow during variation of the line parameters. Hence this surge indicator seems to be sufficiently reliable.

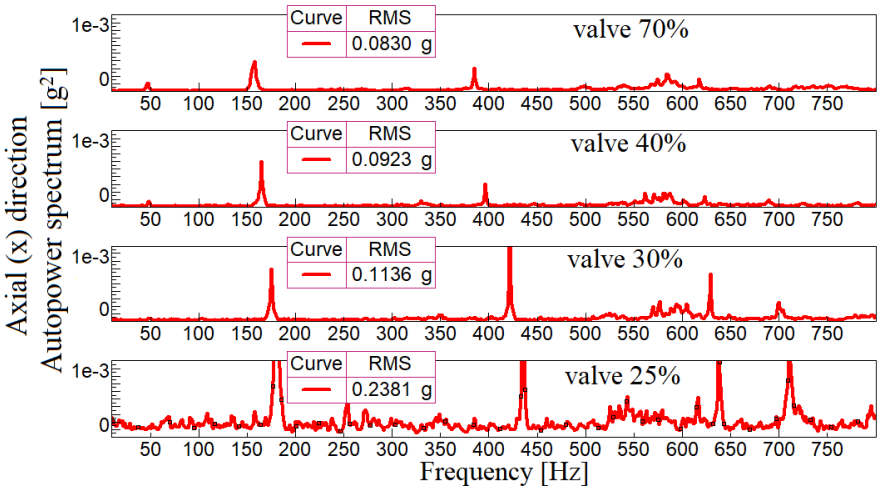

Fig.13 Sub-synchronous auto-power spectrum of accelerometer signal in axial (X red), direction for different values of valve opening and its RMS value (2.3m^3 volume)

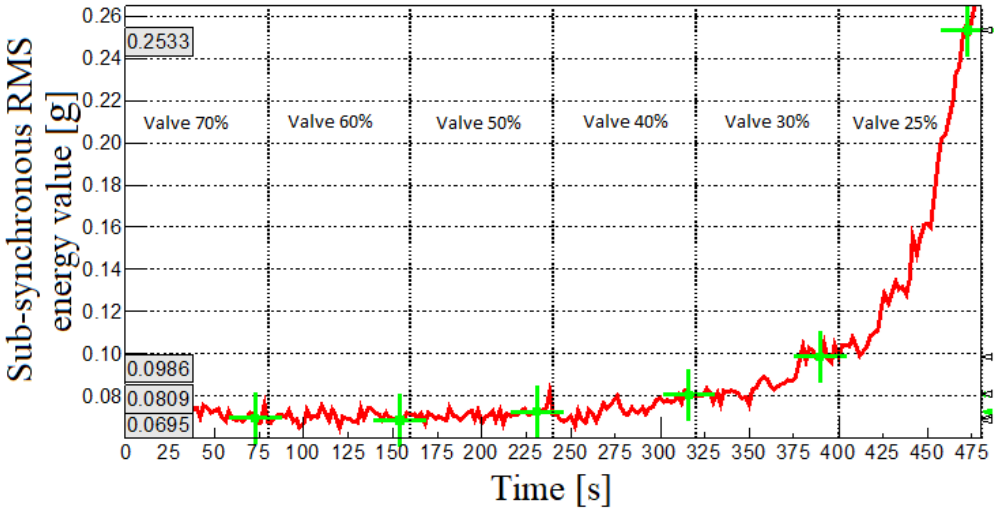

Fig.14 Sub-synchronous RMS energy trend of concatenated X axial signal during the transitory to surge; green crosses are placed at steady-state conditions (values calculated from the 5s extracts)

6. High frequency analysis

Vibration data were also acquired with a high sample frequency (100kHz). So, it was also possible to investigate vibrational and acoustic response in a high frequency band around the blade pass frequency (BPF). Figure 15 shows the auto-power spectrum measured by the accelerometer axial signal on the compressor housing reporting high frequency details in a more stable condition (spectrum above) and immediately before (spectrum below) the surge.

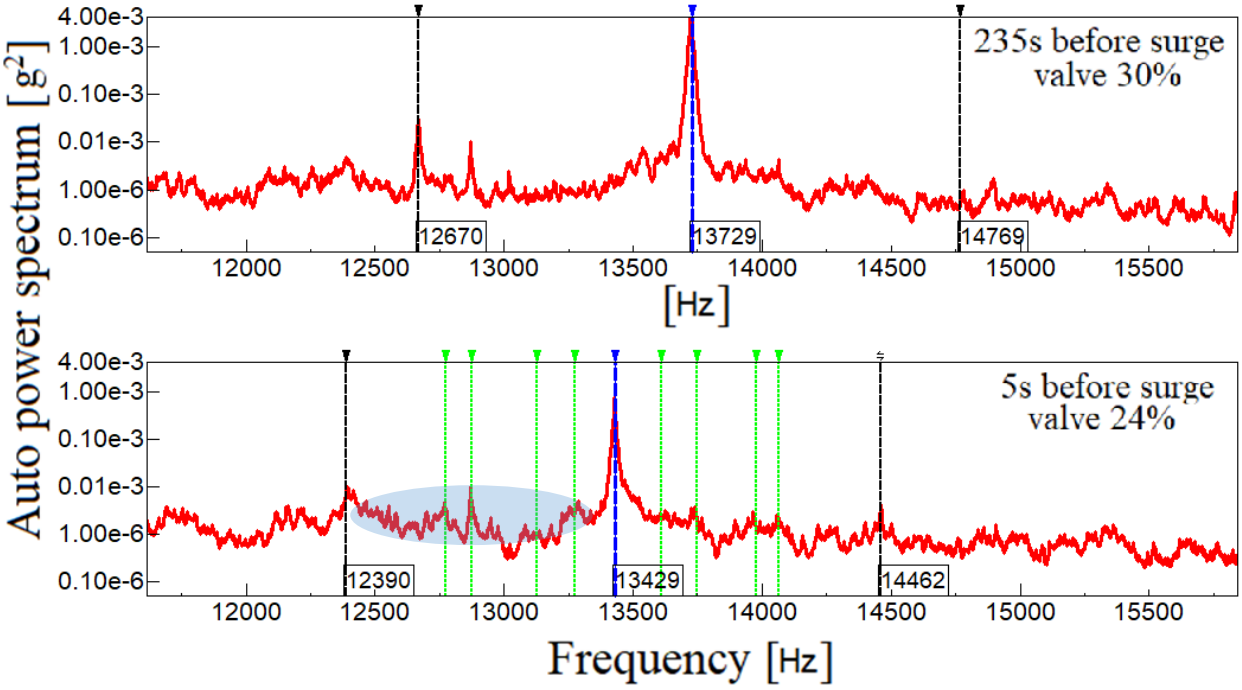

Fig.15 High-frequency accelerometer auto-power spectrum (volume: 2.3m^3)

Blue dotted cursor in both spectra underlines the BPF component which responds to the surge proximity with an energy reduction. Meanwhile there are some significant components (green cursors) that increase their energy near the surge: they are located between the two side bands (black dashed cursors) of the BPF synchronous modulation (BPF-1X and BPF+1X) and so they are sub-synchronous frequencies. These components, although sometimes they are more evident on the left side of BPF (blue ellipse), have their correspondents on the BPF right side due to BPF sub-synchronous modulations.

Based on the theory reported in [33][34] about cyclostationarity in the signals, an idea of deepening the evolution of high-frequency modulations to the surge was matured. Cyclic spectral coherence was calculated from signal intervals far from and immediately before the surge event (a time window of 5s before surge): it is a transformation that searches for modulating cyclic frequencies α in all signal frequencies f. So, it is a non-dimensionalised energy density that shows which energy spectrum frequencies are modulated by some α. Figure 16 shows an example of cyclic spectral coherence colour map: modulating frequencies are in the axis of the abscissas (α cyclic frequency) while spectrum frequencies are in the axis of the ordinates.

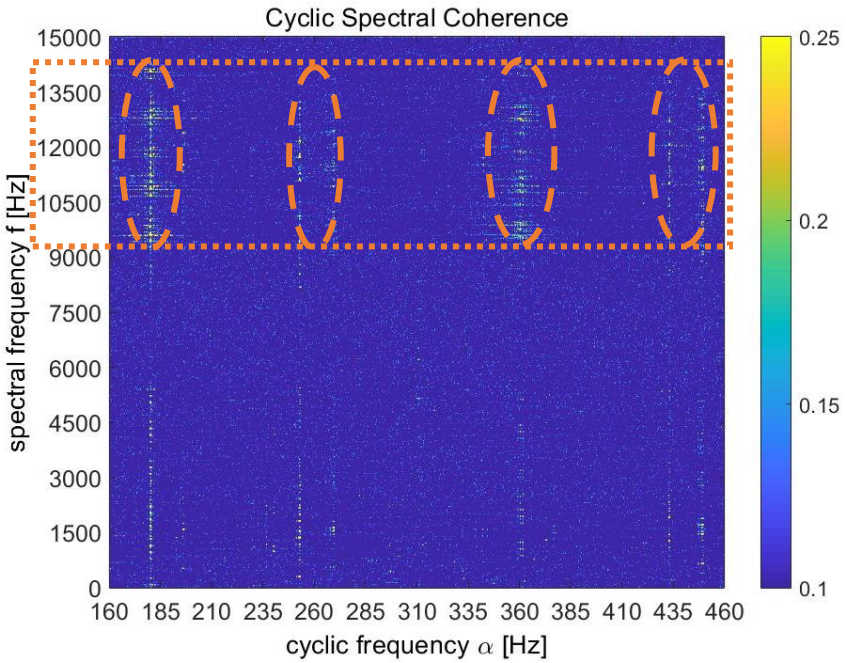

Fig.16 Cyclic spectral coherence calculated from an extract immediately before surge

As shown in the colour map (orange dotted contours), near the surge a range of frequencies around the BPF (9.5kHz-14.5kHz) is involved in more modulation.

To better analyse this behaviour, one tried to calculate the cyclic modulation spectrum which provides the energy of the cyclic components modulating a frequency range Δf of the signal spectrum. The signal was filtered in a band between 9.5X and 14.5X orders of the machine speed frequency and then an energy time frequency analysis was computed on the filtered signal Hilbert envelope. Figure 17 represents a colour map plot of the signal Hilbert envelope time frequency analysis: for each time during the transitory to the surge, it shows the energy of the modulation frequency components.

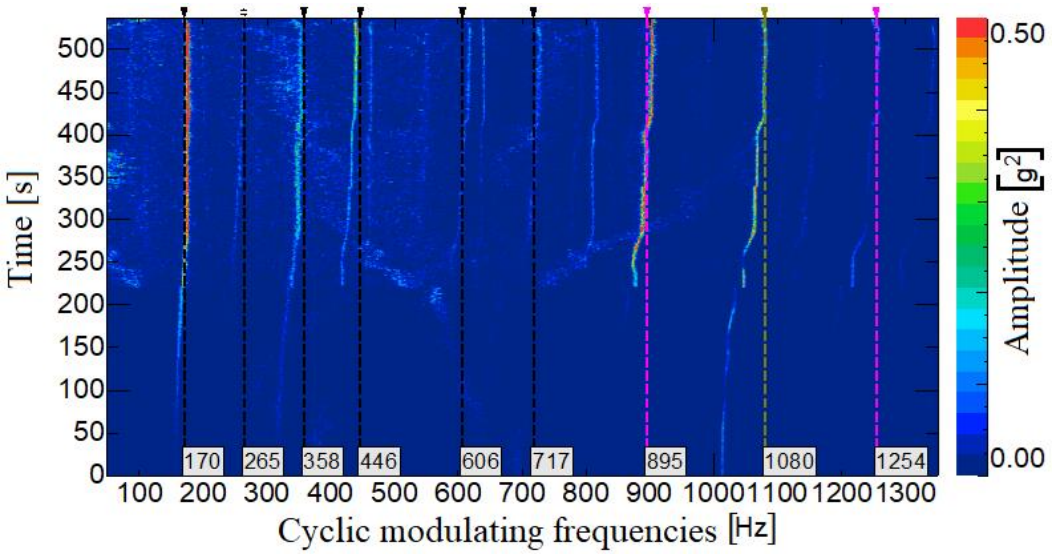

Fig.17 Cyclic modulation spectrum in function of time during surge transient

As can be expected, high frequencies are modulated with machine rotational speed (orange dotted cursor) and its side bands (purple dotted cursors), but there are some sub-synchronous modulations (black dotted cursors) which increase their energy during the transitory to surge. These modulation components are near to those found from resonance research: the incipient surge can create sub-synchronous broadband noise which excites sub-synchronous resonances with the result of a high-frequency band modulation in a range around the BPF between 9.5X-14.5X orders. Both the BPF component energy reduction and the energy increase of the BPF modulations could be useful as surge precursors.

7. Envelope spectrum analysis

After the analysis of signals spectrum content and its energy evolution, another surge precursor could be obtained measuring the loss of the signal spectrum stationarity. From the same 5s intervals used to study different valve closure regimes, 19 consecutive auto-power spectra were calculated (one every 0.25s with a Hanning window with 0.25s). From every set of 19 spectra corresponding to a different valve configuration, mean spectrum, upper and lower envelope spectra and variance spectrum were computed. Compared to previous works [8], auto-power spectrum was preferred instead of the spectrum because attention was focused only on the energy amplitude of frequency contents and, the spectrum being a complex value, the mean of different consecutive complex signal spectra could be affected by phase changes.

As shown in Figure 18 for the 2.3m^3 volume configuration, the energy differences between the two envelope spectra or between an envelope and the mean spectrum increase before the surge: this implies that there is a lack of spectrum stationarity before the surge event.

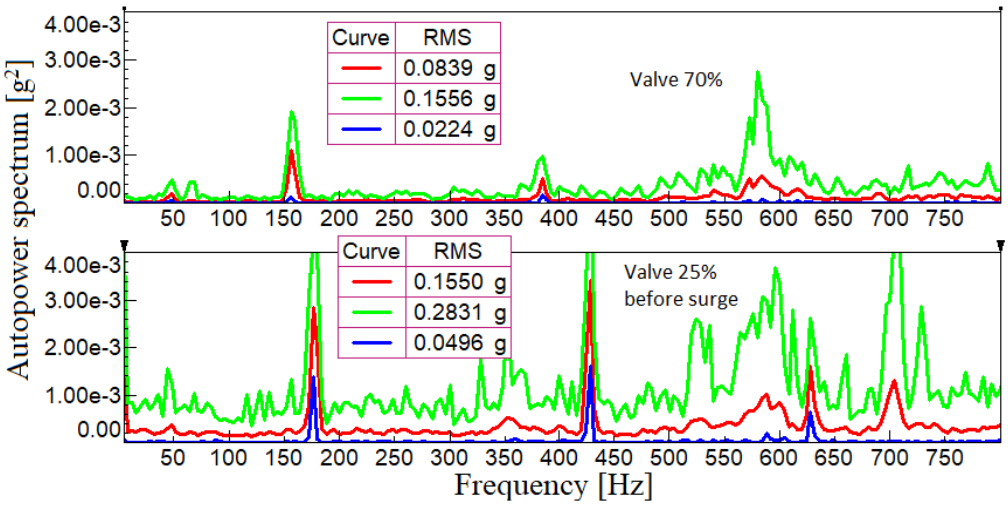

Fig.18 Mean (red), lower envelope (blue), upper envelope (green) spectra of axial accelerometer signal far (valve opened 70%) and immediately before (valve 25%) the surge (volume of 2.3m^3)

This phenomenon can be quantified by sub-synchronous RMS energy value of the variance spectrum which seems to increase before the instability of the surge in all volume configurations. In Figure 19 some variance auto-power spectra are plotted from far from (red spectrum_valve70%) to near (green spectrum_valve25%) the surge event.

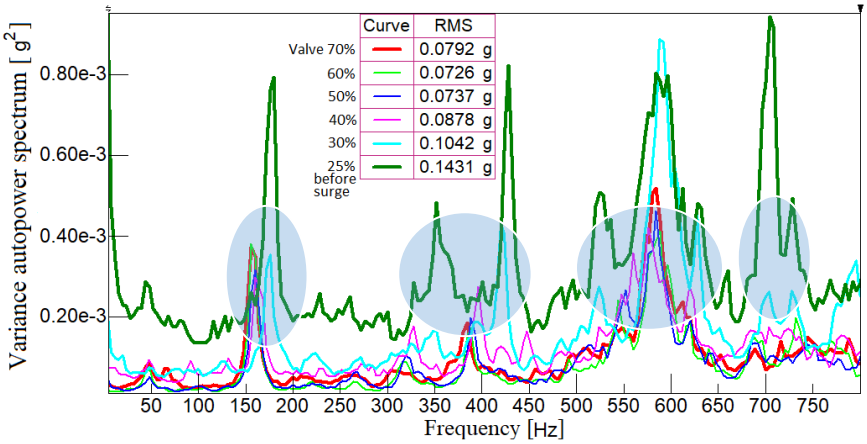

Fig.19 Variance auto-power spectra of the accelerometer axial signal for different valve closures and their sub-synchronous RMS values (volume of 2.3m^3)

Blue ellipses in figure 19 underline that spectrum variations, so the variances are higher in correspondence with the possible structural resonances previously found. Surge incipience produces broadband noise which excites some structural resonances in proximity of the surge so the spectrum variance also has higher amplitude at the resonance frequencies. It is possible to obtain a surge precursor considering the sub-synchronous RMS energy value of spectrum variance: Figure 20 shows its trend in the three different volume configurations in function of the valve closure progressively to the surge.

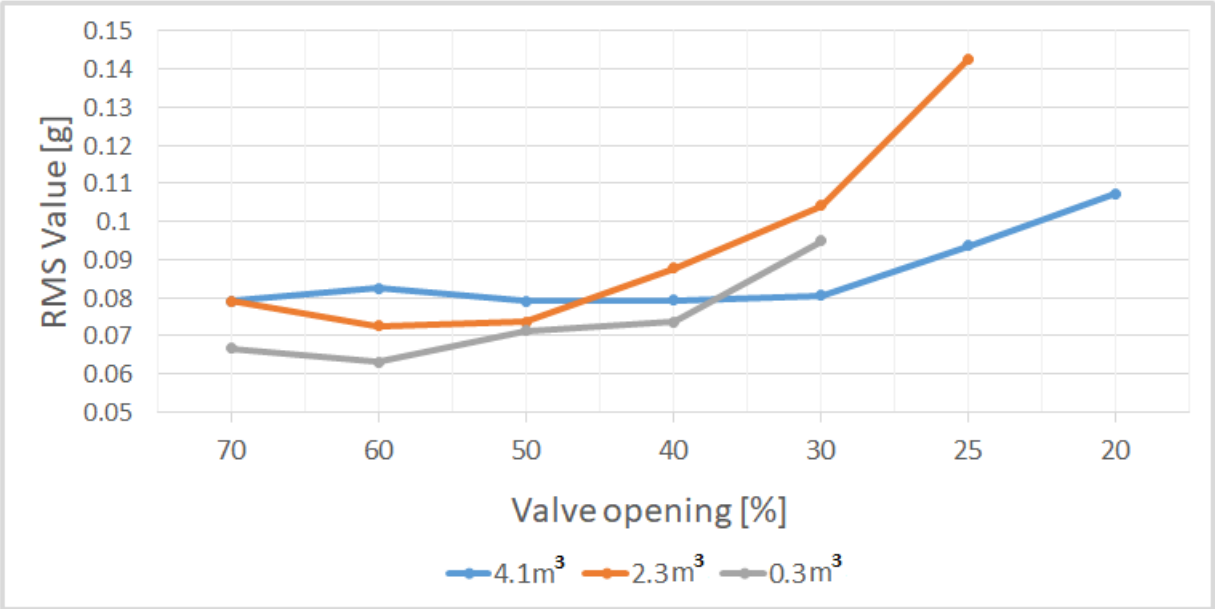

Fig.20 Sub-synchronous RMS energy value trends of spectrum variance

A similar result was obtained analysing axial accelerometer spectrum high frequencies around the blade pass frequency in a band wide enough to contain its possible sub-synchronous modulations. In Figure 21, lower (blue) and upper (green) envelope spectra are plotted together with the average spectrum in a range around the BPF far (above_valve30%) and near (below_valve24%) the surge condition. Black dotted cursor indicates the BPF content while the grey cursors indicate the side bands due to the machine speed synchronous modulation. Considering these content peaks in the three colour spectra, their differences in amplitude increase near the surge (see blue elliptical cursors), so the incipience of the surge also reduces the spectrum stationarity at these high frequencies.

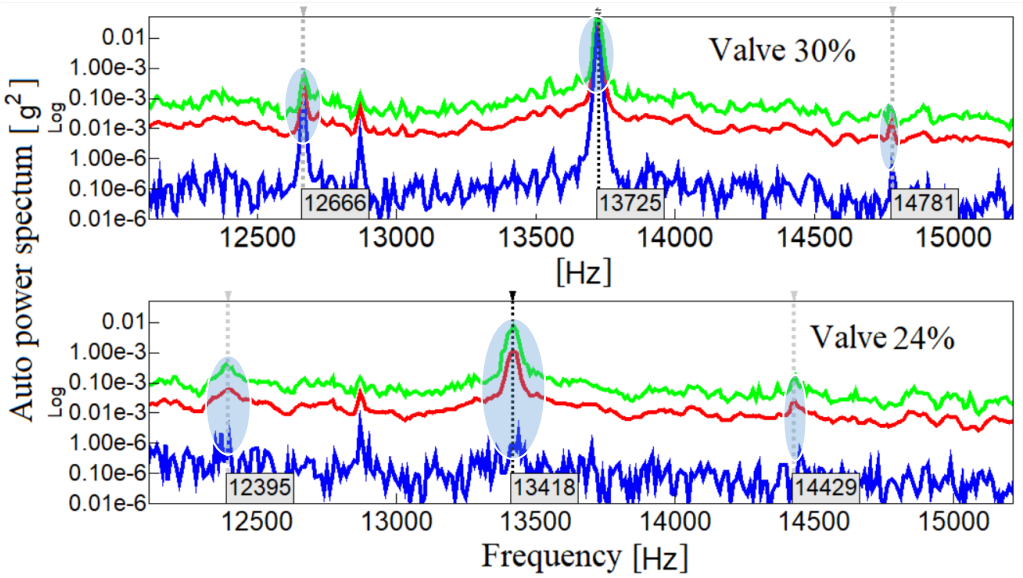

Fig.21 Mean (red), lower envelope (blue), upper envelope (green) spectra of axial accelerometer signal far (valve opened 30%) and immediately before (valve 24%) the surge (volume of 2.3m^3)

In these spectra, the energy reduction of the BPF content is also visible. So, to appreciate the lack of spectrum stationarity through the calculation of variance spectrum RMS energy value is necessary to non-dimensionalise this value with the BPF energy content. Figure 22 shows the non-dimensionalised variance spectrum of accelerometer signal far from (above_valve30%) and right next to (below_valve24%) the surge: in both the spectra BPF content (red dotted cursor) and its side bands are present, but thanks to the lack of spectrum stationarity the variance spectrum amplitude near the surge is higher than it is far from the latter. A similar behaviour is visible in its non-dimensional RMS energy value.

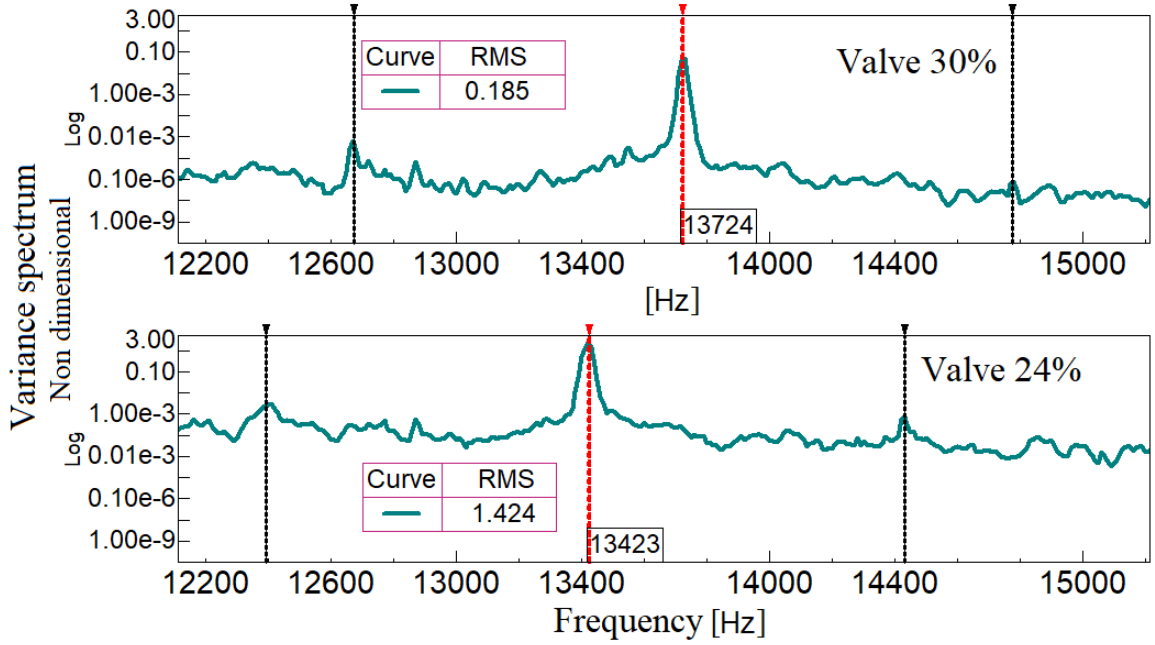

Fig.22 Non-dimensional variance spectrum from accelerometer on the compressor casing in axial direction and its high-frequency RMS value

8. Angle domain analysis

Another surge precursor based on the lack of signal stationarity and repetitiveness could be related to signals in the angle domain. Having a tachometer signal synchronous with the other vibrational acquisition, it was possible to convert signals in function of time to signals in function of the rotation angle of the shaft. Since incipient surge seems to influence sub-synchronous range of frequency content, accelerometer signals of 5s different valve position extracts were filtered between 5 and 800Hz.

Inside of each 5s interval, the signal was converted in function of angle and then cut every 10 cycles (10 rotations of 360°), thus obtaining 350 consecutive trends of signal corresponding to 10 rotation cycles. The length of 10 cycles of shaft rotation was chosen because it permits one to contain numerous sub-synchronous periodicities (if shaft rotates with a frequency of 1,000Hz, it permits one to show periodicity over 100Hz). Despite the adoption of Butterworth filter with cut-off frequency lower than rotational frequency (800Hz), the signal contains a fundamental frequency residue that can be useful as a reference with respect to the occurrence of noise and non-synchronous periodicity (without covering them with its higher energy thanks to the filter).

Figure 23 represents 20 of the consecutive 10-cycle intervals in the 5s extract far from the surge (valve 70%) on the left and near the surge on the right. As shown in the 5s near the surge filtered sub-synchronous 10-cycle intervals differ more from their average than far from the surge. The average is characterised exclusively by synchronous contributions related to the rotation of the shaft

because it is calculated from traces with the same angular reference and that last the same entire number of cycles. So, if the surge incipience increases the sub-synchronous component and noise in the signal, traces will differ more from their mean.

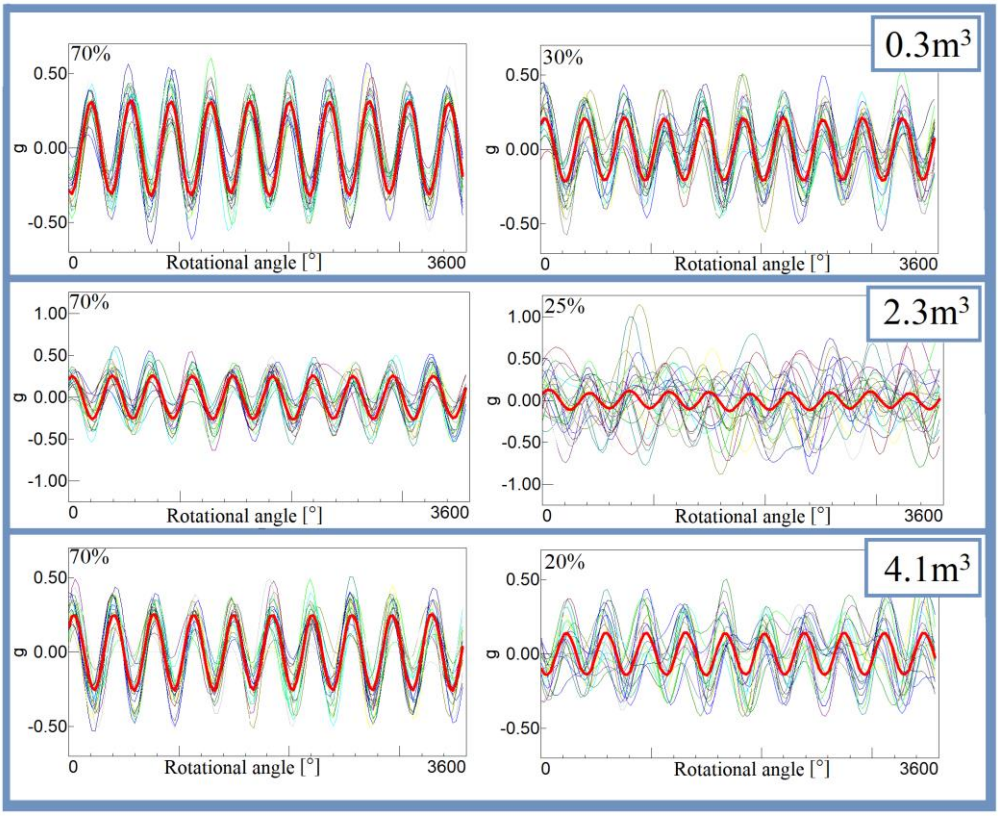

Fig.23 Filtered 10-cycle signal intervals of 5s extracts far from (valve 70%, left) and before the surge (right): the thicker red one is the average of 350 intervals inside the 5s extract

For these reasons, the difference between a generic trace and the mean trace is considered representative of all the non-synchronous contributions of the vibratory response of the system.

Moreover, Figure 24 shows the mean trace (red), the difference between a trace and the mean (green) and the variance trace (blue) for a condition far from (above) and a few instants before surge (below).

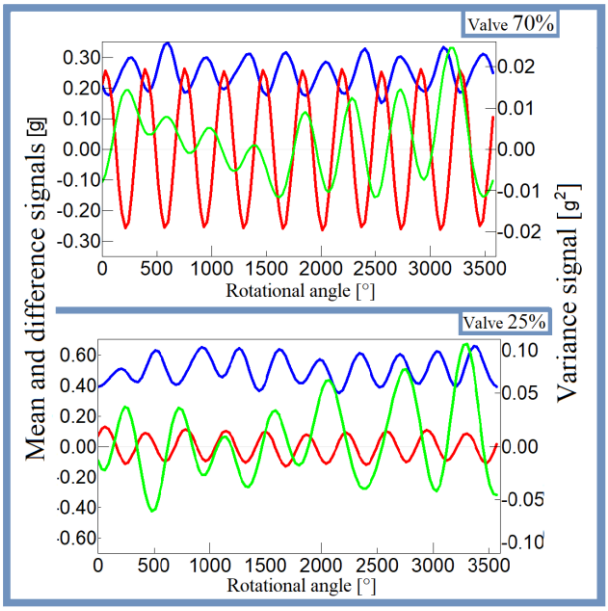

Fig.24 Mean (red), difference (green) and variance (blue) of 10-rotational-cycle axial accelerometer signals (volume of 2.3m^3)

In both graphs of Figure 24, the mean signal has the same periodicity as the residual 1X component synchronous with the rotational speed. So, it has exactly 10 cycles like the number of rotations used to cut the accelerometer signal. Near the surge, synchronous 1X component was at a higher frequency: so, in the graph it has a lower amplitude due to the filter action. Green traces are the differences between a generic trace (between the 350 taken) and the mean trace. It has a slower periodicity probably because it contains all remaining non-synchronous contents. Far from the surge, difference signals have lower amplitude and present 8 peaks, probably due to the 1X order lower side band. Near the surge they have a higher amplitude and a slower periodicity: 1X order lateral bands remain out of filter pass band and there is a significant increase of other lower frequency contents.

Blue traces are the variance, with respect to the average, of 350 consecutive traces lasting 10 rotational cycles. Calculating the variance of 350 signal traces is equivalent to removing all the self-excited vibrations related to the rotation of the machine from the signal to obtain the average energy of all non-synchronous contents which are considered more imputable to phenomena linked to the fluid. Variance periodicities are increased by elevation to the square, but the variance trace RMS energy value seems to be a useful precursor since it increases near the surge. Figure 25 shows the 350-interval variance signal and its RMS value from different valve closure: 5s extracts from far to the last valve position before the surge event for different plant-volume configurations.

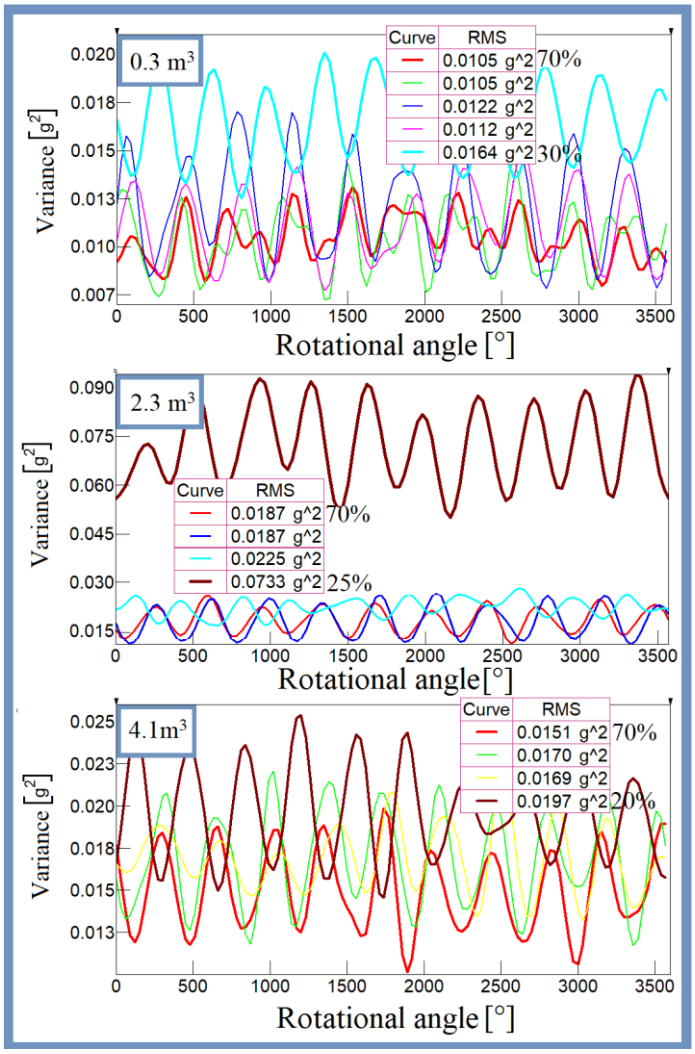

Fig.25 Sub-synchronous variance signal of 350 intervals of 10 cycles and its RMS energy value for different valve closure conditions from far from (valve 70%) to a condition close to the surge event

A similar angle domain analysis was carried out using a micro accelerometer signal in axial direction, to study the high frequency contents around the blade pass frequency. Inside the same 5s intervals, used to calculate the variance spectrums for the low frequencies, shorter 1s intervals were chosen where machine rotation speed had the most constant trend (and the closest to surge in the interval near to the surge). 1s intervals were filtered with an order band pass filter between 9X and 14.5X of rotation frequency and converted to angle domain. Then they were cut every 2 cycles thus obtaining 350 consecutive trends of signal corresponding to 2 rotations of 360°. The length of 2-cycle shaft rotation was chosen because it permits us to contain some cycles of all frequency contents in the filter band. As done before, from every set of 350 consecutive trends the average synchronous accelerometer signal was calculated and then the difference and the signals variance with respect to the average. In Figure 26, spectra of the average synchronous accelerometer signal are plotted for a stable condition (red) and immediately before surge (green).

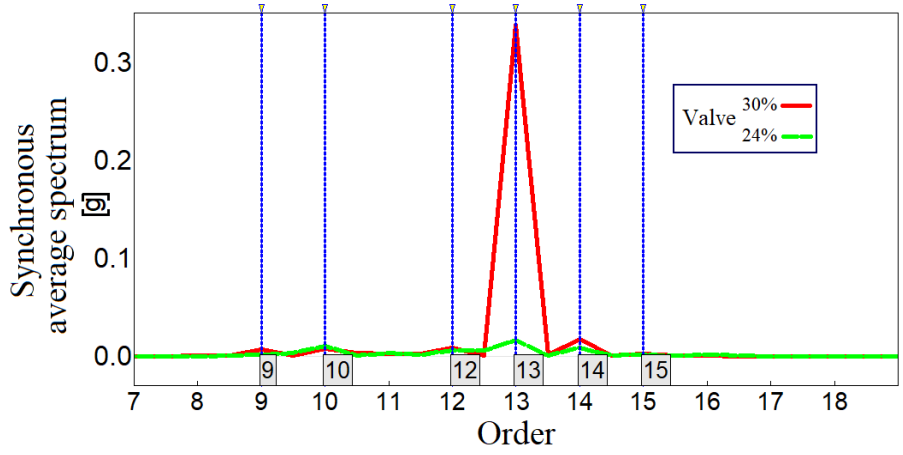

Fig.26 Average synchronous accelerometer spectrum from 350 traces lasting 10 cycles, far (red) and immediately before the surge (green) (volume of 2.3 m^3)

Average spectrum plot, being obtained from signal traces converted to the angle domain with the same phase reference (k-phasor), has the frequency axis represented by the machine revolution speed orders and it is limited to the range around the BPF of the pass band filter used. This kind of synchronous average seems mostly to highlight the BPF component behaviour which has a higher amplitude far from the surge than immediately before. As for the sub-synchronous analysis, also for the high-frequency differences between each of 350-set traces and their mean was calculated to study the instability of signal and the possible non-synchronous contributions presence. Figure 27 shows two auto-power spectra which are the mean of 350 difference auto-power spectra from a set far (red) and immediately before the surge (green).

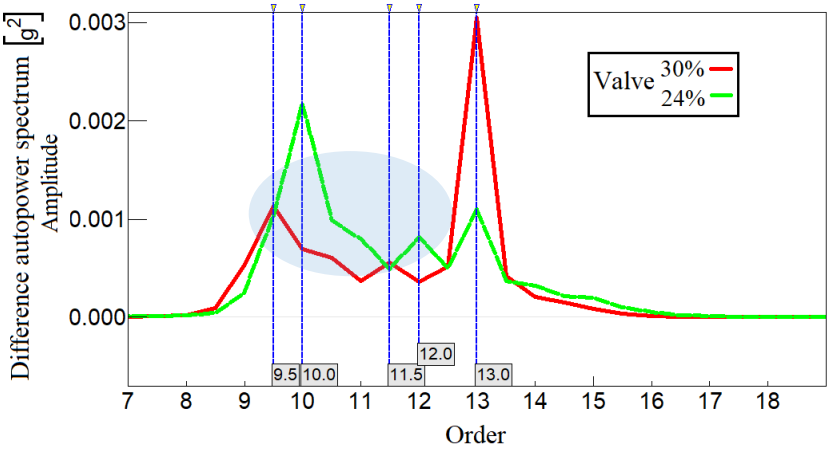

Fig.27 Mean difference auto-power spectra from sets in a stable condition far from (red) and a few instants before surge (green) (volume of 2.3m^3)

Far from the surge also the difference spectrum has a peak at the BPF which decreases near the surge. BPF content oscillations probably depend on percentage from its amplitude. In the difference spectrum, near the surge, content of other orders, lower than BPF, seems to increase their energy

probably due to some instable fluid dynamic behaviour with time period a little higher than that of the BPF.

In the end, a single variance trend was obtained from every set of 350 trends corresponding to a different valve position. Moreover, Figure 28 shows that the RMS energy value of the variance trend also increases approaching the surge for the content of the signal around the blade pass frequency and so it could be useful for surge prediction.

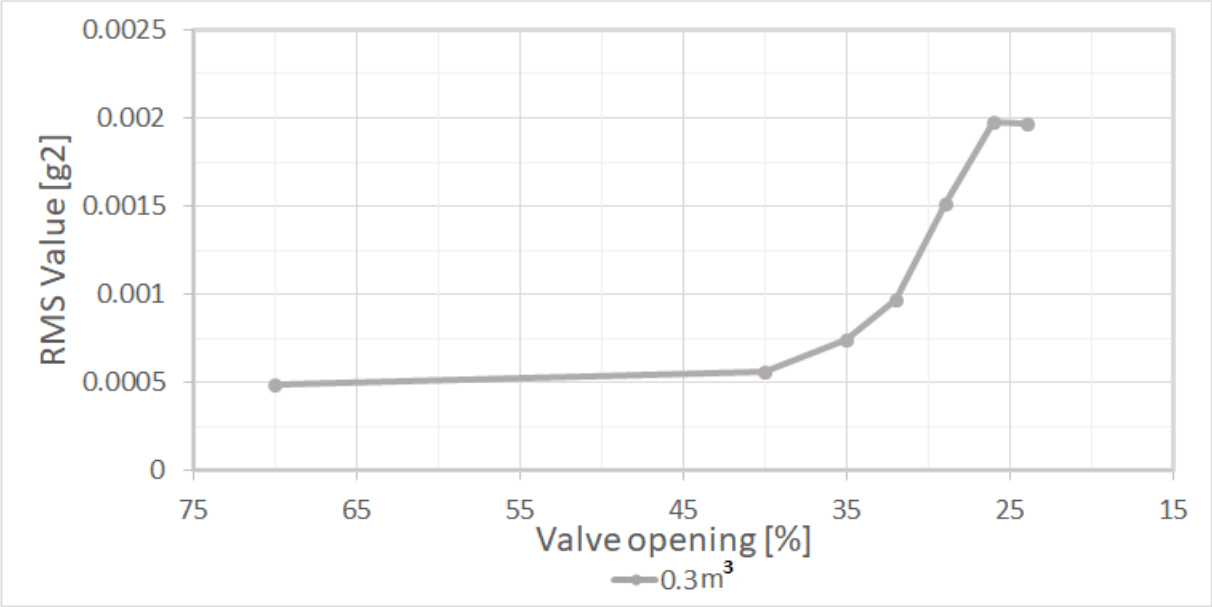

Fig.28 RMS energy value for different valve closure conditions of high-frequency variance signal (order 9X-14.5X) of 350 intervals of 2 cycles (volume of 0.3 m^3)

9. Conclusions

This paper evaluates the possibility of obtaining diagnostic information for incipient surge detection from accelerometer and microphone signals analysis [35][36] in the case of a turbine connected with large volumes. A large test campaign was carried out with an experimental facility including a T100 microturbine connected with a modular vessel (to change the volume size) between the recuperator outlet duct and the combustor inlet line. Surge phenomenon was generated progressively closing a valve placed in the air path, increasing the pressure loss. In the following points, the main results are listed for different signal processing techniques in time, frequency and angle domain:

- This activity showed that a complete system dynamic characterisation is useful to improve the diagnostic analysis: it permits one both to distinguish in the signals the contents associated with sources different from those of the phenomenon to be diagnosed and to identify possible system resonances. Resonance frequencies seem to be significant for

diagnostic purposes because in the response signals the corresponding components showed a higher sensitivity to the energy of the instability phenomenon. In this activity, system resonance identification was obtained by analysing responses at different operative conditions: run-up, run-down and surge condition generating an impulsive broadband excitation.

- Acoustic and vibrational spectrum energy levels are useful as quantifiers for surge prediction. Significant diagnostic information is present both in the signals' sub-synchronous contents and higher frequencies, in correspondence with the contributions associated with the phenomenon of passage of the blade.
- For diagnostic purposes, it is significant to be able to detect the presence of signal-main-contribution modulations that appear more evident in correspondence with an incipient surge condition. The most significant modulated phenomenon is that of the blade passage. To detect these modulation phenomena, the signal spectra and the calculation of the cyclic coherence function were considered.
- Promising predictions and diagnostic results were obtained through the study of the lack of vibrational and acoustic signal stationarity. The analysis was conducted by adopting a signal representation both in frequency and angle domain. In the first case, the tests showed an increase in the difference between average auto-power spectrum and the envelope auto-power spectrum, both evaluated on a significant number of spectra corresponding to a system operating condition. In the second case, some average functions, representative of system synchronous contributions, were calculated and used as reference to perform a comparison on signal extracts in the angle domain far and near critical operational condition.

It is believed that the signal analysis methods proposed can provide robust indicators useful for a diagnostic system for incipient surge condition identification. The reliability of these indicators was verified for three different volumes connected to the turbine. Although the intermediate volume showed the most sensitivity, acceptable results were obtained for all three volume configurations. These results allow us to generalise indicator applicability regardless of the size of the volume. The results presented above are relative to a microturbine because advanced cycles and innovative plant layouts are (usually conceived for distributed generation) related to this machine size. However, the techniques presented in this paper to find surge precursors could also be, in general, applicable for large-size machines.

In future work, additional quantifiers will be defined applying the previous analysis techniques to the instantaneous pressure signal acquired in the inlet compressor section. Furthermore,

Independent Component Analysis (ICA) [37] and Blind Source Separation (BSS) [38] techniques can be considered to more efficiently extract diagnostic contents from the signals.

Acknowledgements

The authors would like to thank Dr. Matteo Pascenti, laboratory technician at TPG, for his essential activity in test, preparation and management.

The authors declare that they have no conflict of interest.

Nomenclature

Acronyms	
BSS	Blind Source Separation
E. grid	Electrical grid
Ex	heat Exchanger
FFT	Fast Fourier Transform
Auto-power spectrum	
k-phasor	Phase Reference for rotational angle
M	Motor
REC	Recuperator
RMS	Root Mean Square
SOFC	Solid Oxide Fuel Cell
TPG	Thermochemical Power Group
VBE	On/off emergency bleed valve
VM	Main line valve
VO	Modular vessel outlet valve
Variables	
BPF	blade pass frequency [Hz]
N	rotational speed [rpm]
nX	Rotational nth Order
MM	Main line mass flow rate [kg/s]
MR	Modular vessel mass flow rate [kg/s]
PRC1	Recuperator inlet pressure [bar]
TC1	Compressor inlet temperature [K]
TOT	Turbine Outlet Temperature [K]
vol.	Volume [m3]

References

[1] Zaccaria V., Tucker D., Traverso A., “Transfer function development for SOFC/GT hybrid systems control using cold air bypass”, Applied Energy, 165 (2016) 695-706.

[2] Greitzer E.M., “Surge and Rotating Stall in Axial Flow Compressors. Part I: Theoretical Compression System Model”, Journal of Engineering for Power, 98 (1976) 190-198.

[3] Hagino N., Uda K., Kashiwabara Y., “Prediction and Active Control of Surge Inception of a Centrifugal Compressor”, Proceedings of the International Gas Turbine Congress, 2003.

[4] Fanyu L., Jun L., “Stall Warning Approach With Application to Stall Precursor-Suppressed Casing Treatment”, ASME Paper GT2016-58172, ASME Turbo Expo 2016, Seoul, South Korea.

[5] Biliotti D., Bianchini A., Vannini G., Belardini E., Giachi M., Tapinassi L., Ferrari L., Ferrara G., “Analysis of the rotor dynamic response of a centrifugal compressor Subject to aerodynamic loads due to Rotating Stall”, Journal of Turbomachinery ASME 2015, Vol. 137

[6] Bently D. E., Goldman P., “Vibrational Diagnostics of Rotating Stall in Centrifugal Compressors”, ORBIT First Quarter 2000

[7] Cuneo A., Zaccaria V., Tucker D., Sorce A., “Gas turbine size optimization in a hybrid system considering SOFC degradation”, Applied Energy. 230 (2018) 855-864.

[8] Ferrari M.L., Silvestri P., Pascenti M., Reggio F., Massardo A.F., “Experimental Dynamic Analysis on a T100 Microturbine Connected With Different Volume Sizes”, Journal of Engineering for Gas Turbines and Power, 140 (2018) 021701_1-12.

[9] Rossi I., Sorce A., Traverso A., “Gas turbine combined cycle start-up and stress evaluation: A simplified dynamic approach”, Applied Energy, 190 (2017) 880–890.

[10] Arnulfi G.L., Giannattasio P., Giusto C., Massardo A.F., Micheli D., Pinamonti P., “Multistage Centrifugal Compressor Surge Analysis. Part I: Experimental Investigation”, Journal of Turbomachinery. 121 (1999) 305-311.

[11] Arnulfi G.L., Giannattasio P., Giusto C., Massardo A.F., Micheli D., Pinamonti P., “Multistage centrifugal compressor surge analysis: Part II-numerical simulation and dynamic control parameters evaluation. Journal of Turbomachinery”, 121 (1999) 312-320.

[12] Munari E., Morini M., Pinelli M., Spina P.R., Suman A, “Experimental Investigation of Stall and Surge in a Multistage Compressor”, ASME Paper GT2016-57168, ASME Turbo Expo 2016, Seoul, South Korea.

[13] Lis´kiewicz G., Horodko L., Stickland M., Kryłłowicz W., “Identification of phenomena preceding blower surge by means of pressure spectral maps. Experimental Thermal and Fluid Science”, 54 (April 2014) Pages 267-278

[14] Kabral R., Åbom M. “Investigation of turbocharger compressor surge inception by means of an acoustic two-port model” Journal of Sound and Vibration 412 (2018) 270e286

[15] Marelli S., Misley A., Taylor A., Silviestri P., Capobianco M., Canova M., “Experimental Investigation on Surge Phenomena in an Automotive Turbocharger Compressor” SAE Technical Papers, doi: 10.4271/2018-01-0976.

[16] Aretakis N., Mathioudakis K., Kefalakis M., Papailiou K., “Turbocharger unstable operation diagnosis using vibroacoustic measurements”, ASME Journal of Engineering for Gas Turbines and Power,126 (Nov. 2004) pages 840-847

[17] Morini M., Pinelli M., Venturini M., “Acoustic and Vibrational Analyses on a Multi-Stage Compressor for Unstable Behavior Precursor Identification”, ASME Paper GT2007-27040, ASME Turbo Expo 2007, Montreal, Canada.

[18] Munari E., D’Elia G., Morini M., Mucchi E., Pinelli M., Spina P.R., “Experimental Investigation of Vibrational and Acoustic Phenomena for Detecting the Stall and Surge of a Multistage Compressor”, ASME Journal of Engineering for Gas Turbines and Power. 2018; 140(9):092605-092605-9. GTP-17-1451 doi: 10.1115/1.4038765

[19] Ferrari M.L., Pascenti M., Magistri L., Massardo A.F., “MGT/HTFC hybrid system emulator test rig: Experimental investigation on the anodic recirculation system.”, Journal of Fuel Cell Science and Technology, 8 (2011) 021012_1-9.

[20] Lucifredi A., Noceti D., Ferraro A., Silvestri P., Ortenzio G., “Acoustic and vibrational characterization for noise reduction of a Piaggio P180 cockpit blower” (2011) 8th

International Conference on Condition Monitoring and Machinery Failure Prevention Technologies 2011, CM 2011/MFPT 2011, 1, pp. 254-264.

[21] Craig R. R., Kurdila A. J., “Fundamentals of structural dynamics” John Wiley edition, New Jersey - USA, 2006

[22] Lucifredi A., Silvestri P. “An overview of fundamental requirements for a condition monitoring and fault diagnosis system for machinery and power plants” (2003) Proceedings of the Tenth International Congress on Sound and Vibration, pp. 4691-4698.

[23] Oppenheim A.V., Schafer R.W., “Discrete-time signal processing”, Prentice-Hall, Inc. Upper Saddle River, NJ, USA, 1999

[24] Harris C.M., Piersol A. G., “Harris’ Shock and vibration handbook”, McGraw-Hill, New York, 2002, ISBN 0-07-137081-1

[25] Vance J. M. “Rotordynamics of Turbomachinery” Wiley-Interscience Hoboken, NJ, USA, ISBN: 978-0-471-80258-7, 1988

[26] Friswell M. I., Penny J. E. T., Garvey S. D., Lees A. W., “Dynamics of Rotating Machines”

[27] Muszyńska A., “Rotordynamics”, CRC Press, Taylor & Francis Group, ISBN 978-0-8247-2399-6, 2005

[28] Bendat J. S., Piersolauth A. G., “Random Data Analysis and Measurement Procedures”

[29] Jin D., Haupt U., Hasemann H., Rautenberg M., “Excitation of blade vibration due to surge of centrifugal compressors”, ASME International Gas Turbine and Aeroengine Congress and Exposition, Cologne Germany 1992

[30] Vakakis A. F., “Non-linear normal modes (nnms) and their applications in vibration theory: an overview”, Mechanical Systems and Signal Processing (1997) 11(1), 3-22

[31] Kerschen G., Peeters M., Golinval J.C., Vakakis A.F., “Nonlinear Normal Modes, Part I: A Useful Framework for the Structural Dynamicist”, Mechanical Systems and Signal Processing 23, (2009), 170-194

[32] Nuttall A. H., “Spectral Estimation by Means of Overlapped Fast Fourier Transform Processing of Windowed Data”, Naval Underwater System Center Report No. 4169

[33] Antoni J., “Cyclostationarity by examples”, Mechanical Systems and Signal Processing 23, (2009) 987–1036

[34] Antoni J., “Cyclic spectral analysis in practice”, Mechanical Systems and Signal Processing 21, (2007) 597–630

[35] Lucifredi A., Silvestri, P., Tripepi, F. “Development of criteria for vibration qualification of mechanical components through lms test lab mission synthesis software” (2010) 7th International Conference on Condition Monitoring and Machinery Failure Prevention Technologies 2010, CM 2010/MFPT 2010, 1, pp. 578-589.

[36] Aonzo E., Lucifredi A., Silvestri P. “Diagnostic modules based on chaos theory for condition monitoring of rotating machinery” (2000) Proceedings of the 25th International Conference on Noise and Vibration Engineering, ISMA, pp. 937-944.

[37] Hyvärinen A., Karhunen J., Oja E., “Independent component analysis”, John Wiley & Sons, Inc.

[38] Comon P., Jutten C., “Handbook of Blind Source Separation Independent Component Analysis and Applications”, Elsevier Ltd.

Figure 1

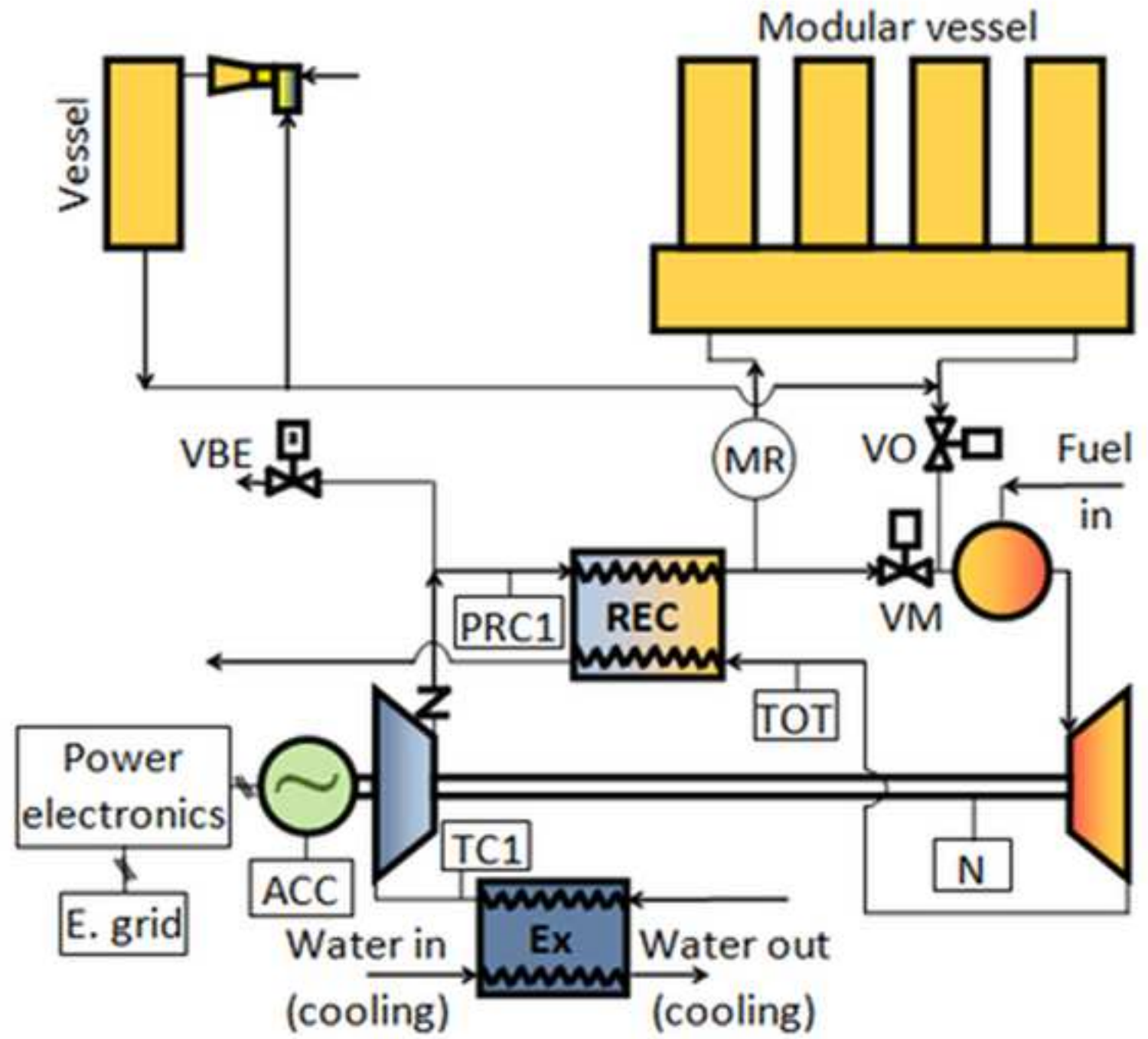

Figure 2

Click here to access/download;Figure;Figure 2.tif

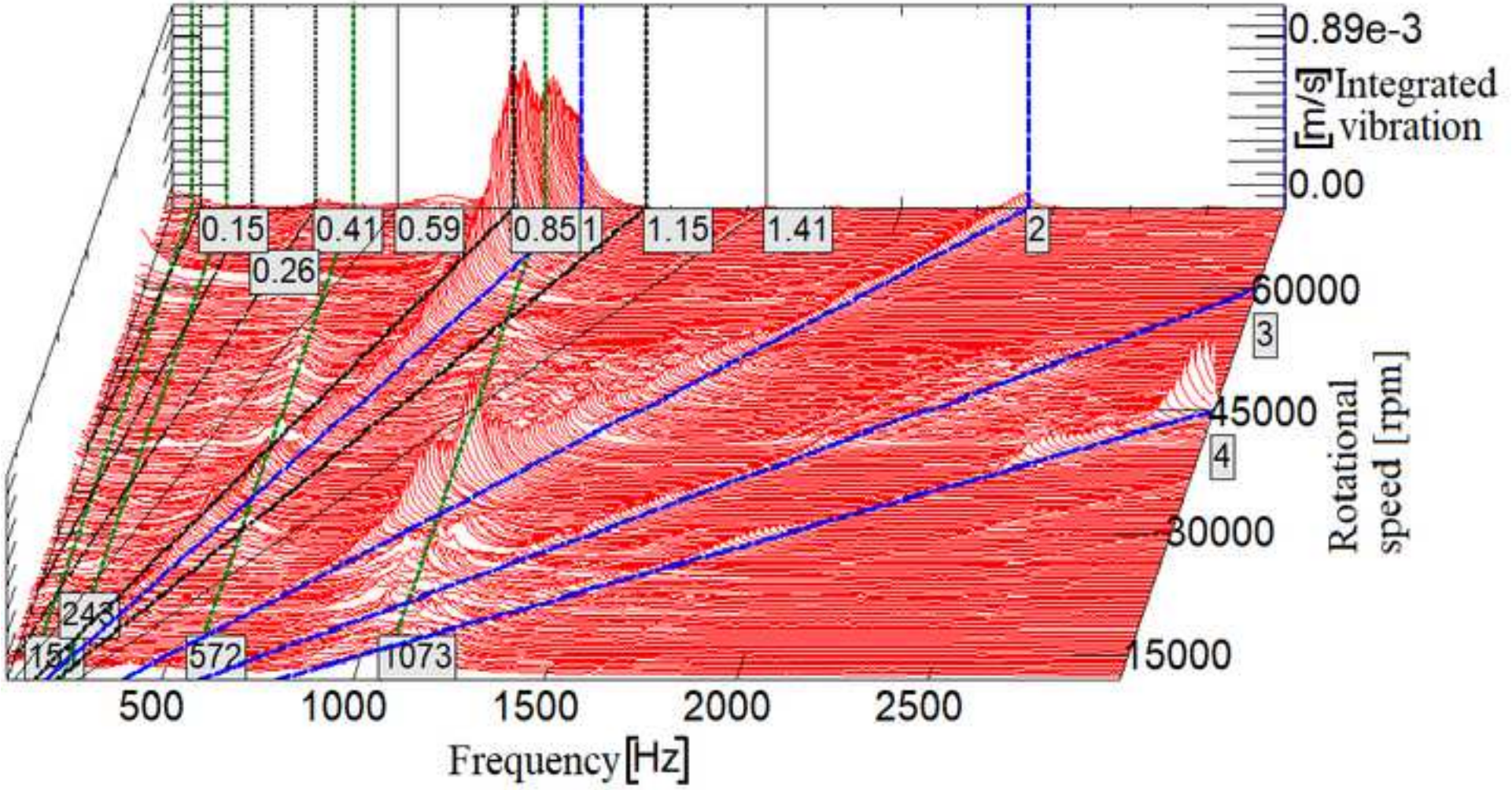

Figure 3

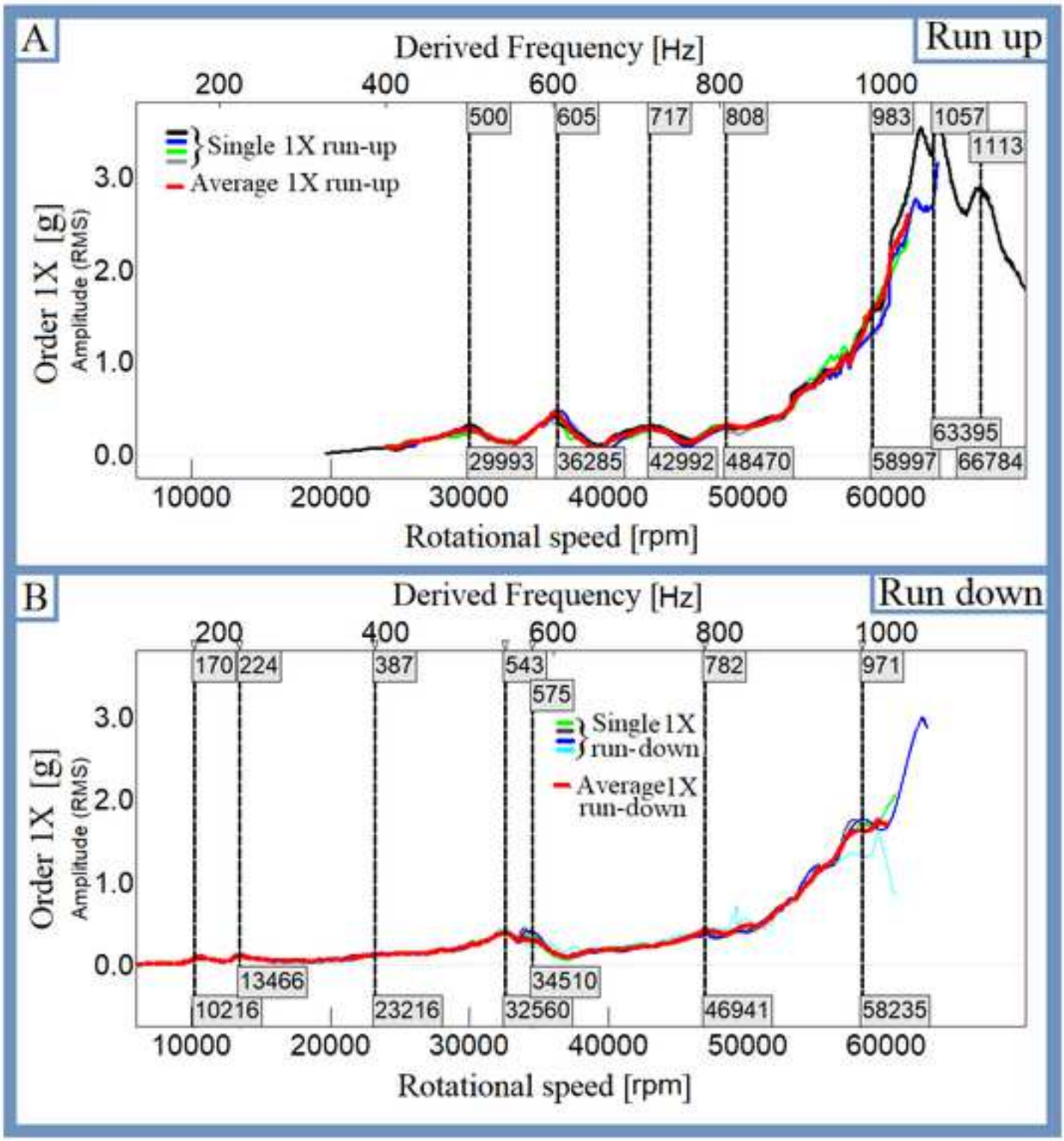

Figure 4

Click here to access/download;Figure;Figure 4.tif

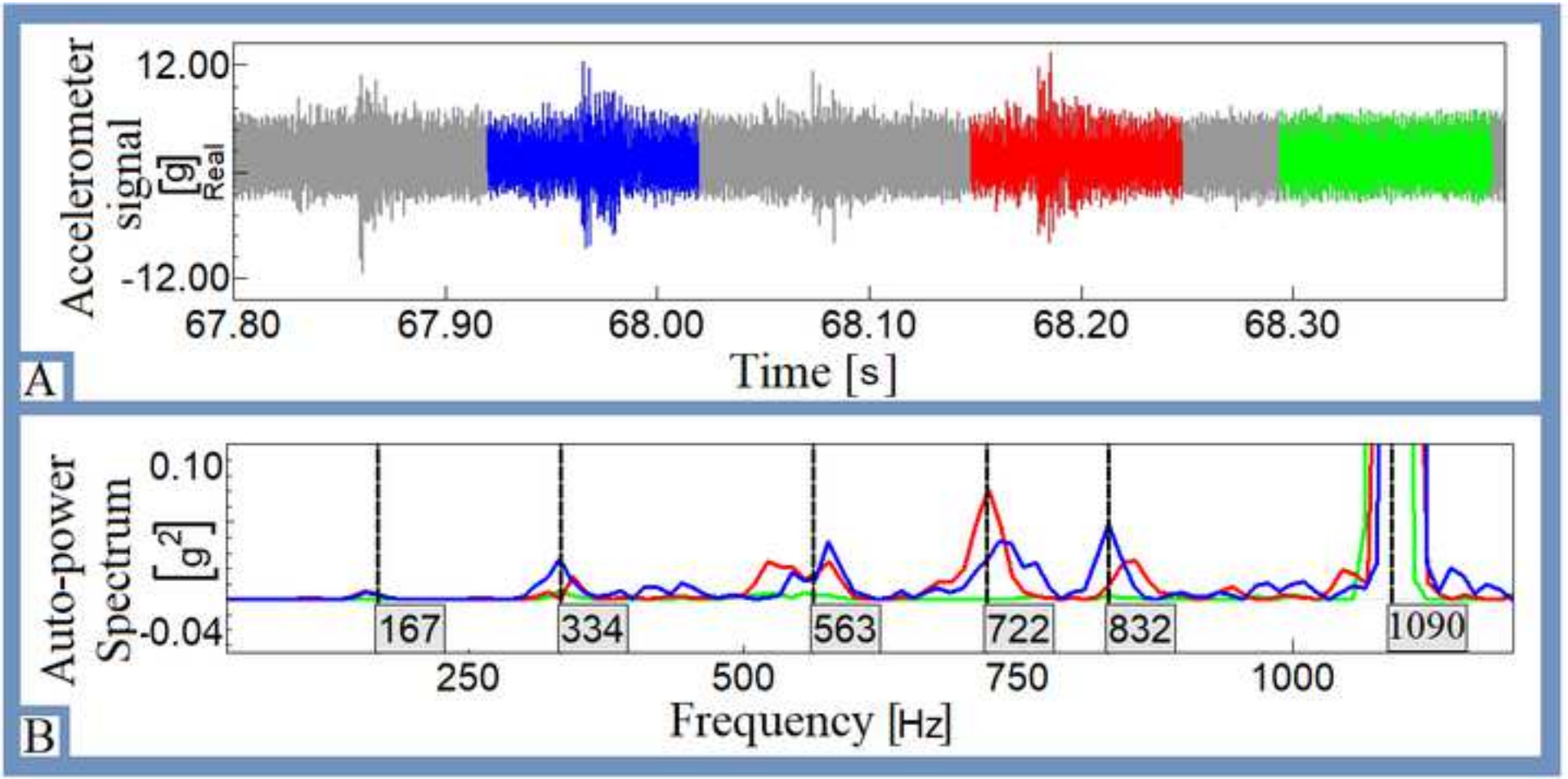

Figure 5

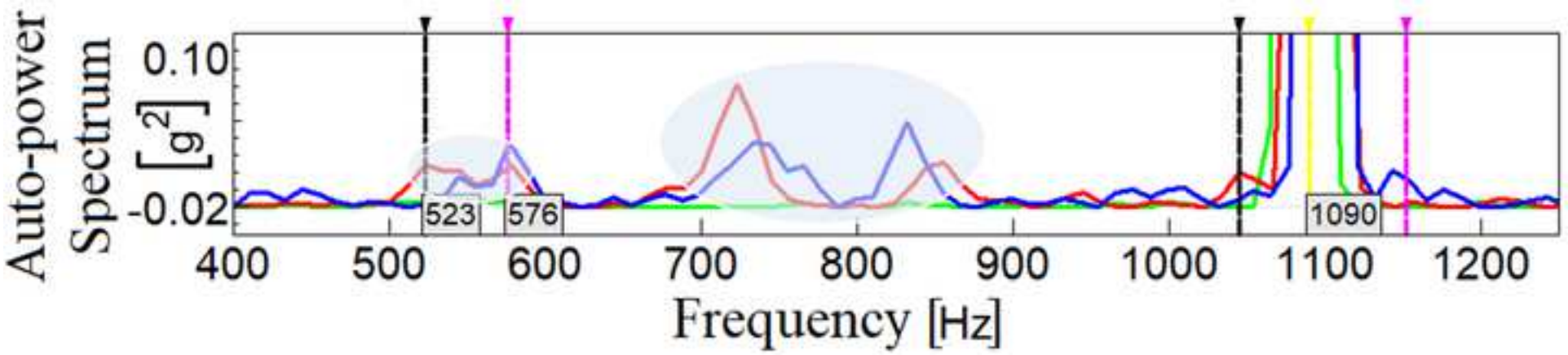

Figure 6

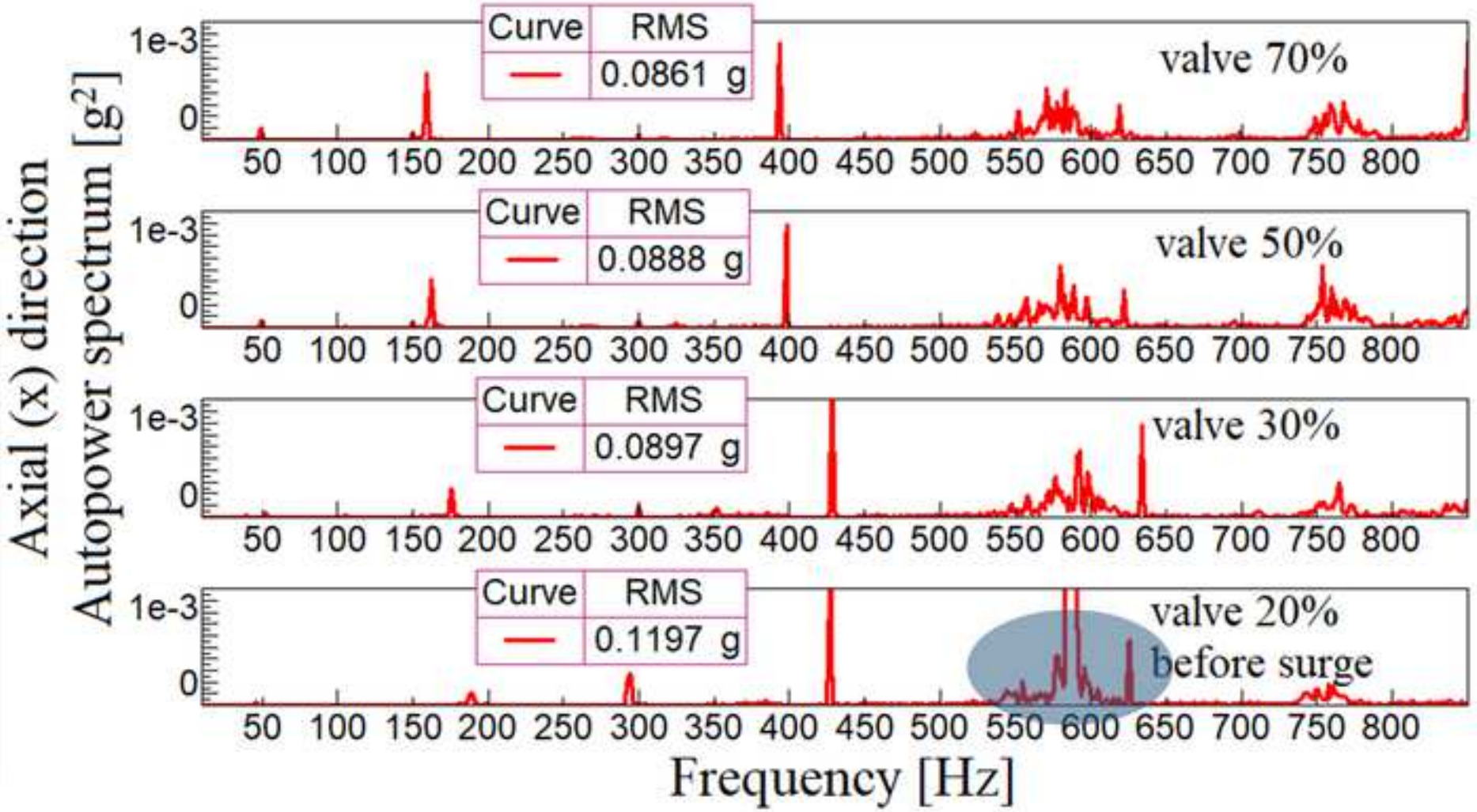

Figure 7

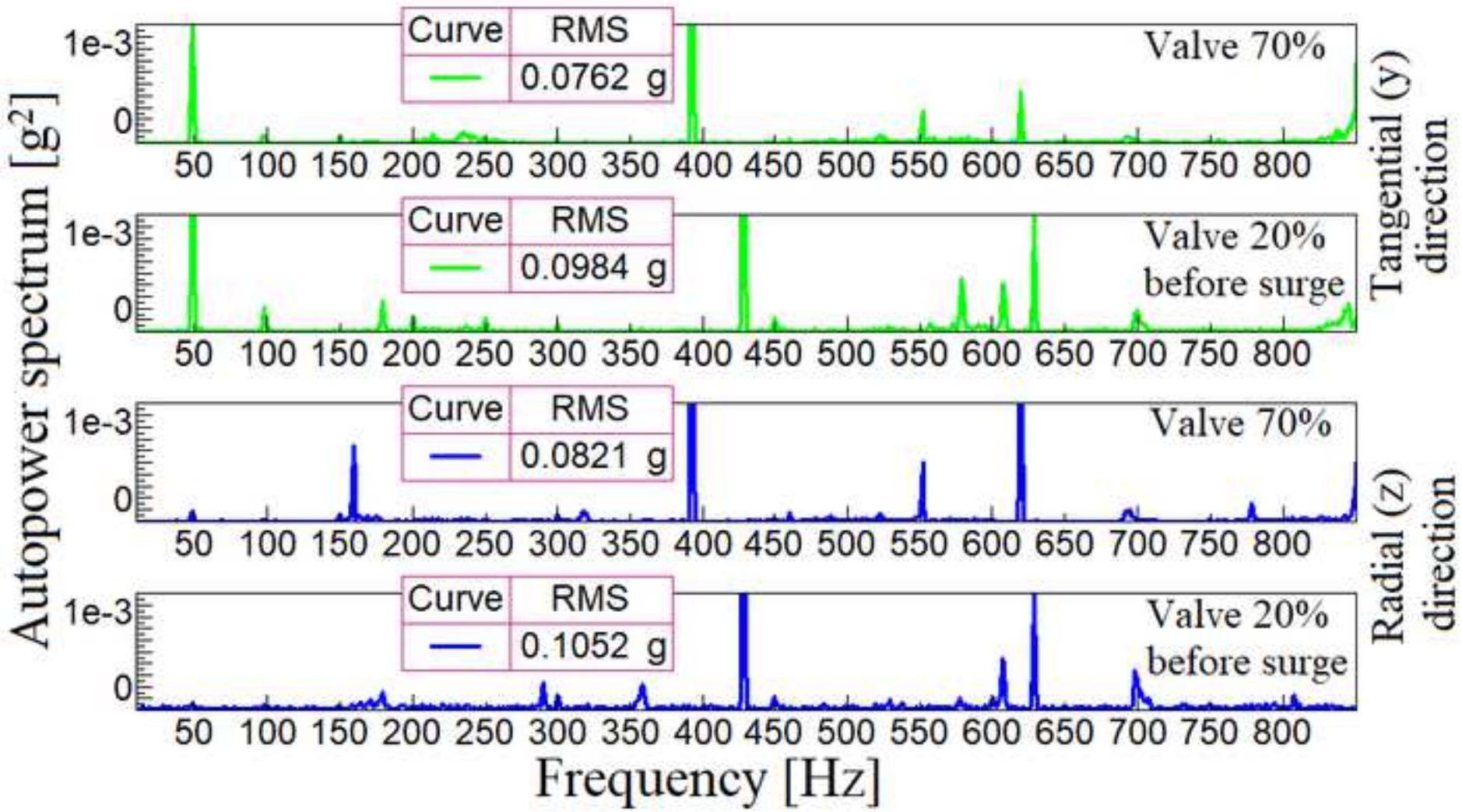

Figure 8

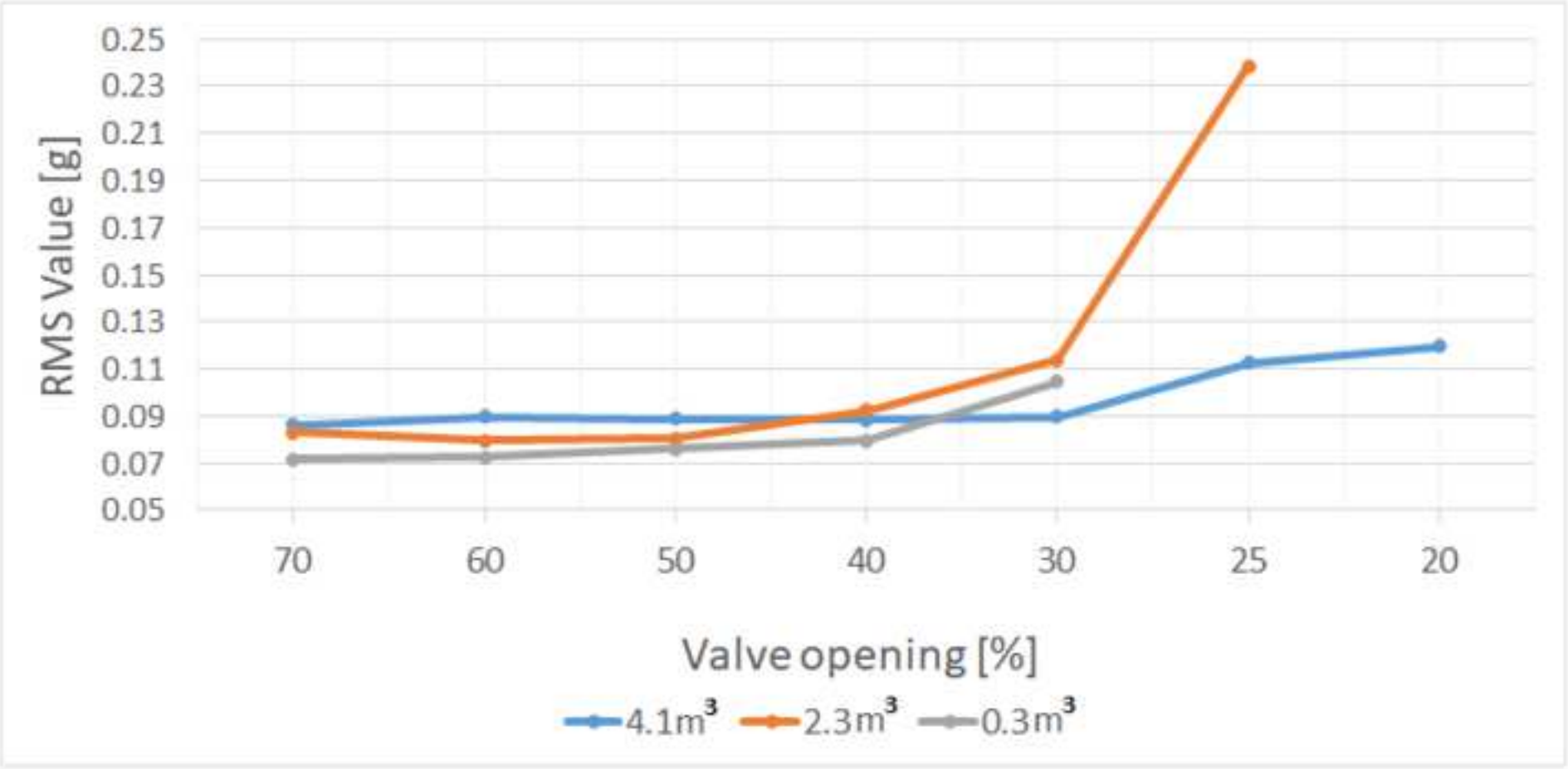

Figure 9

Click here to access/download;Figure;Figure 9.tif

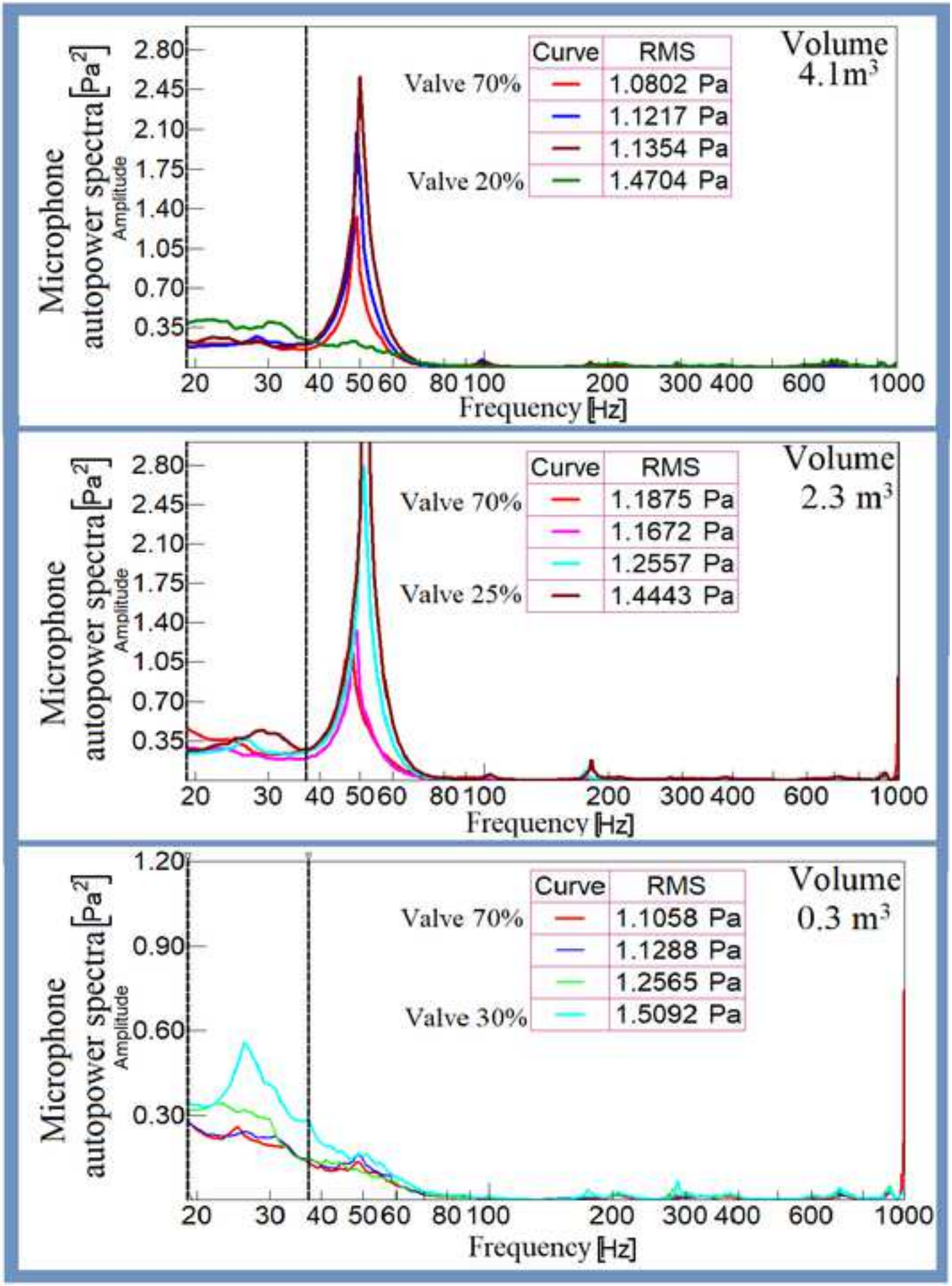

Figure 10

Click here to access/download;Figure;Figure 10.tif

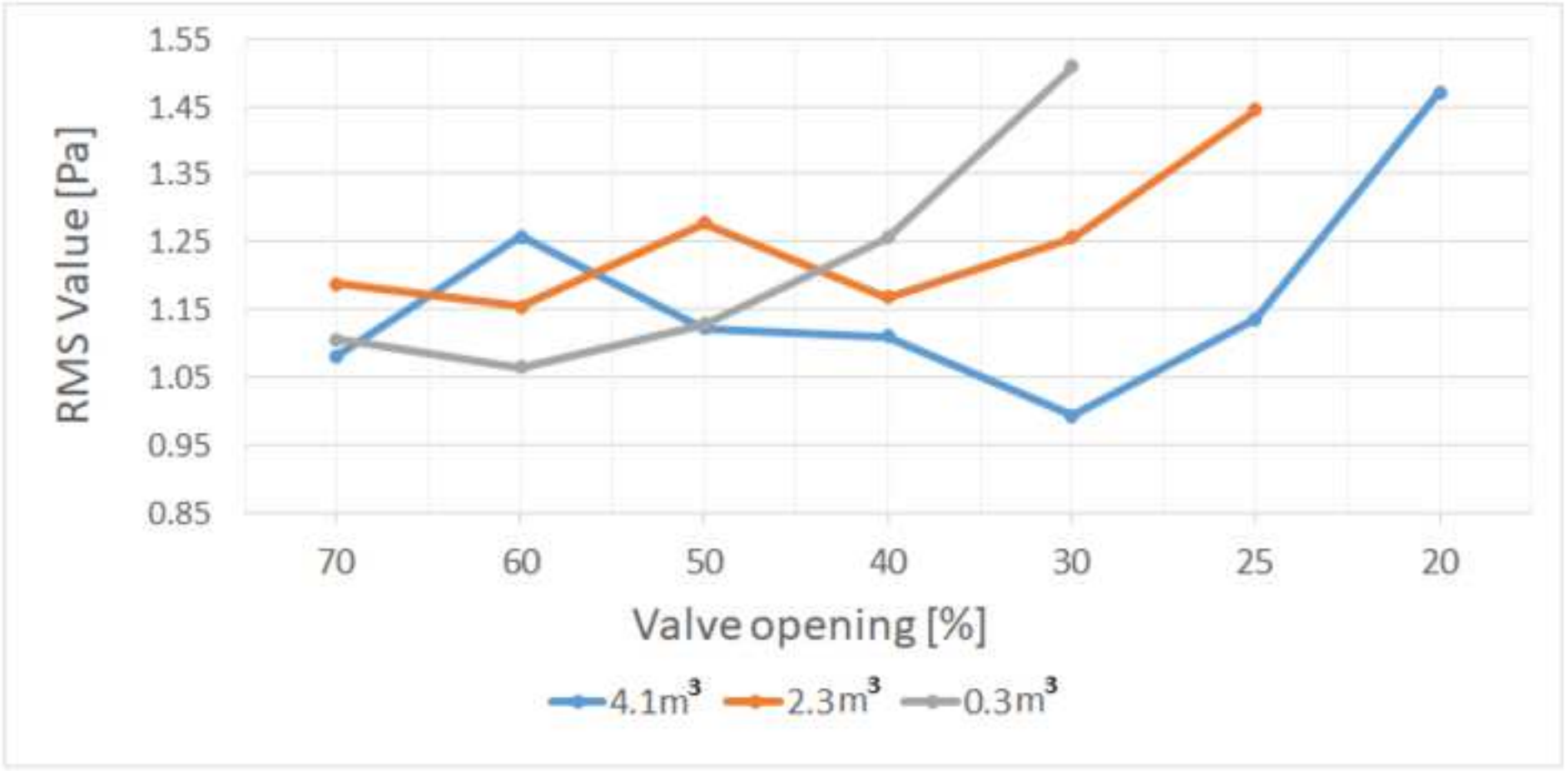

Figure 11

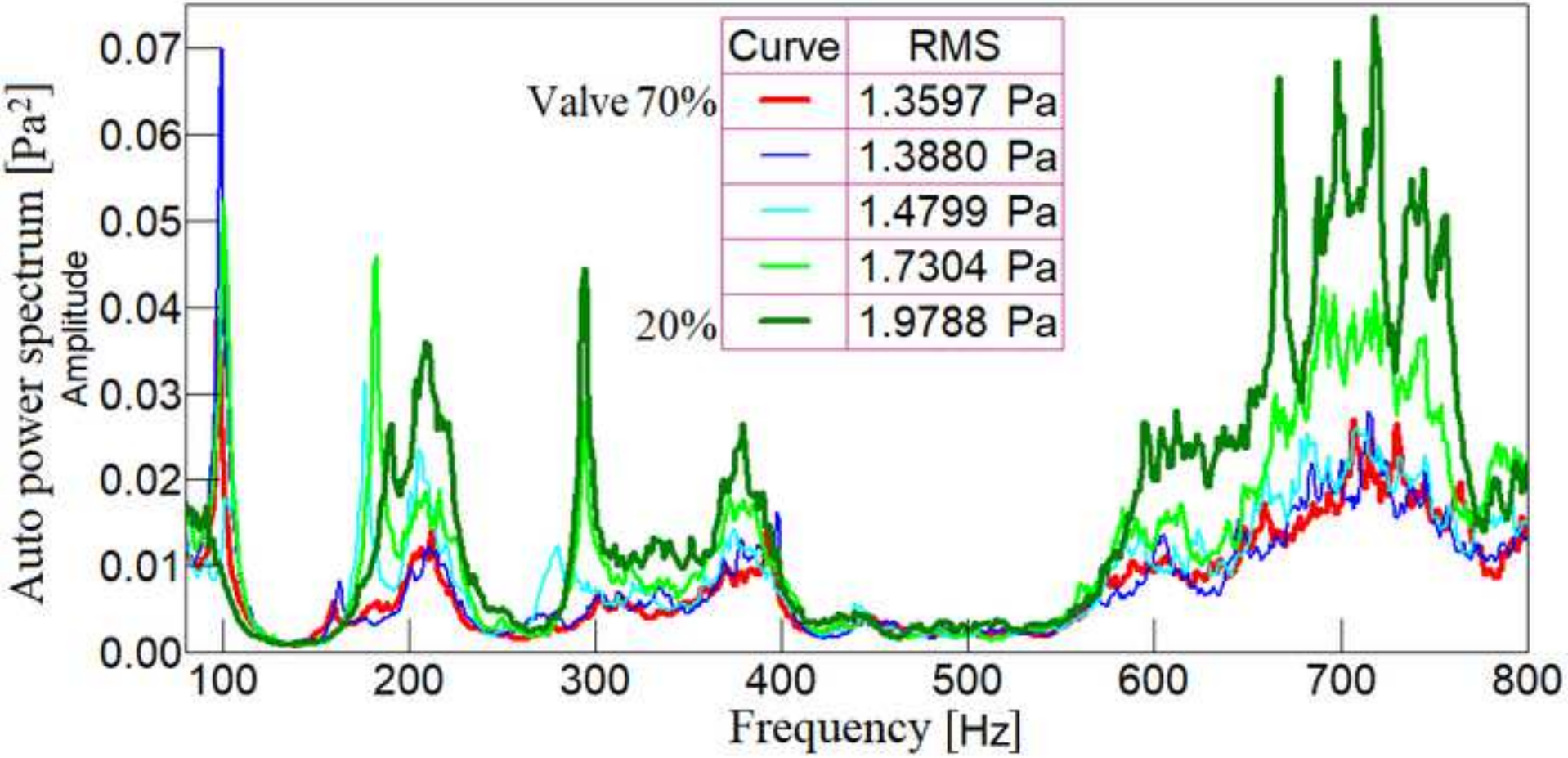

Figure 12

Click here to access/download;Figure;Figure 12.tif

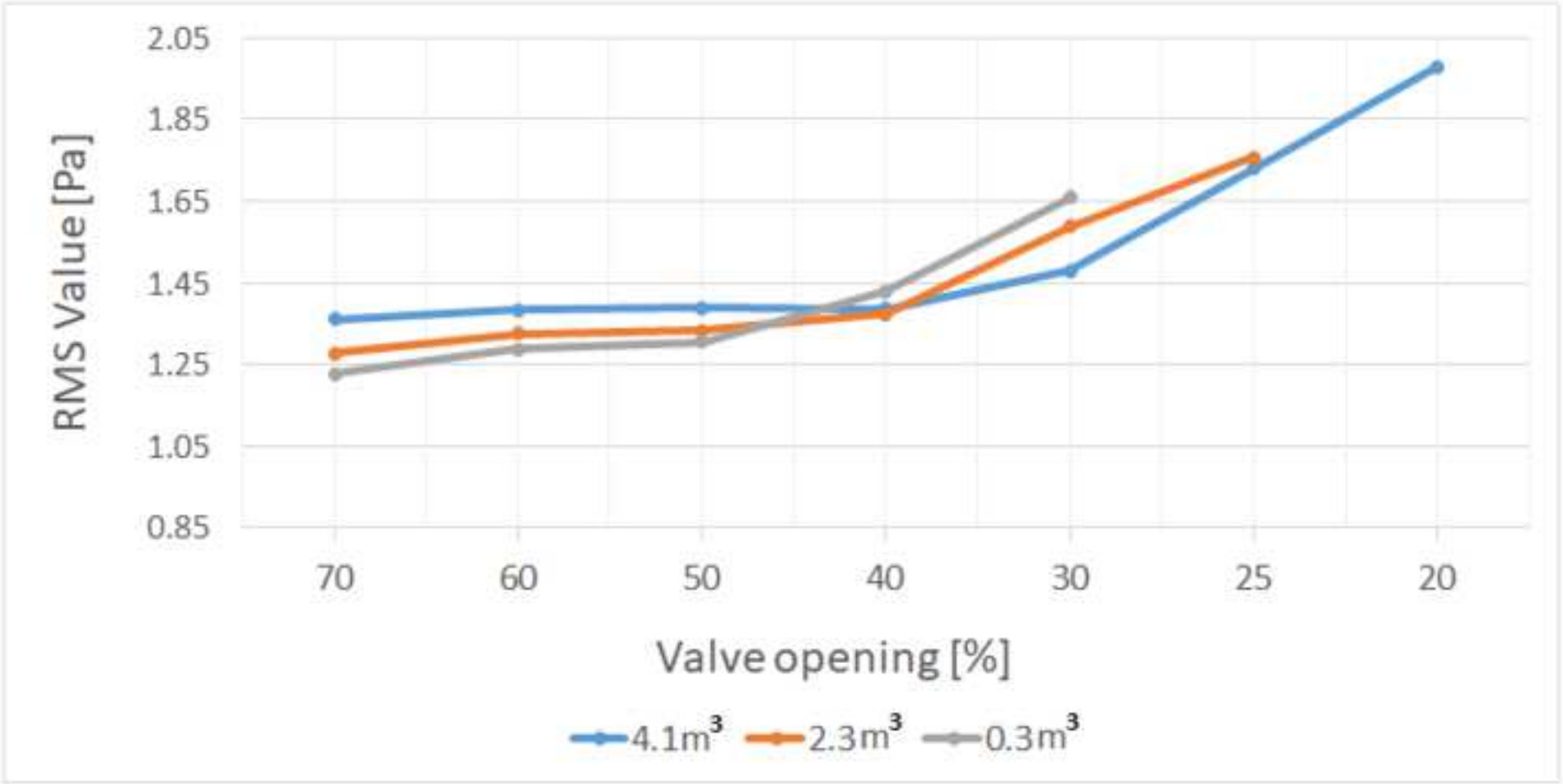

Figure 13

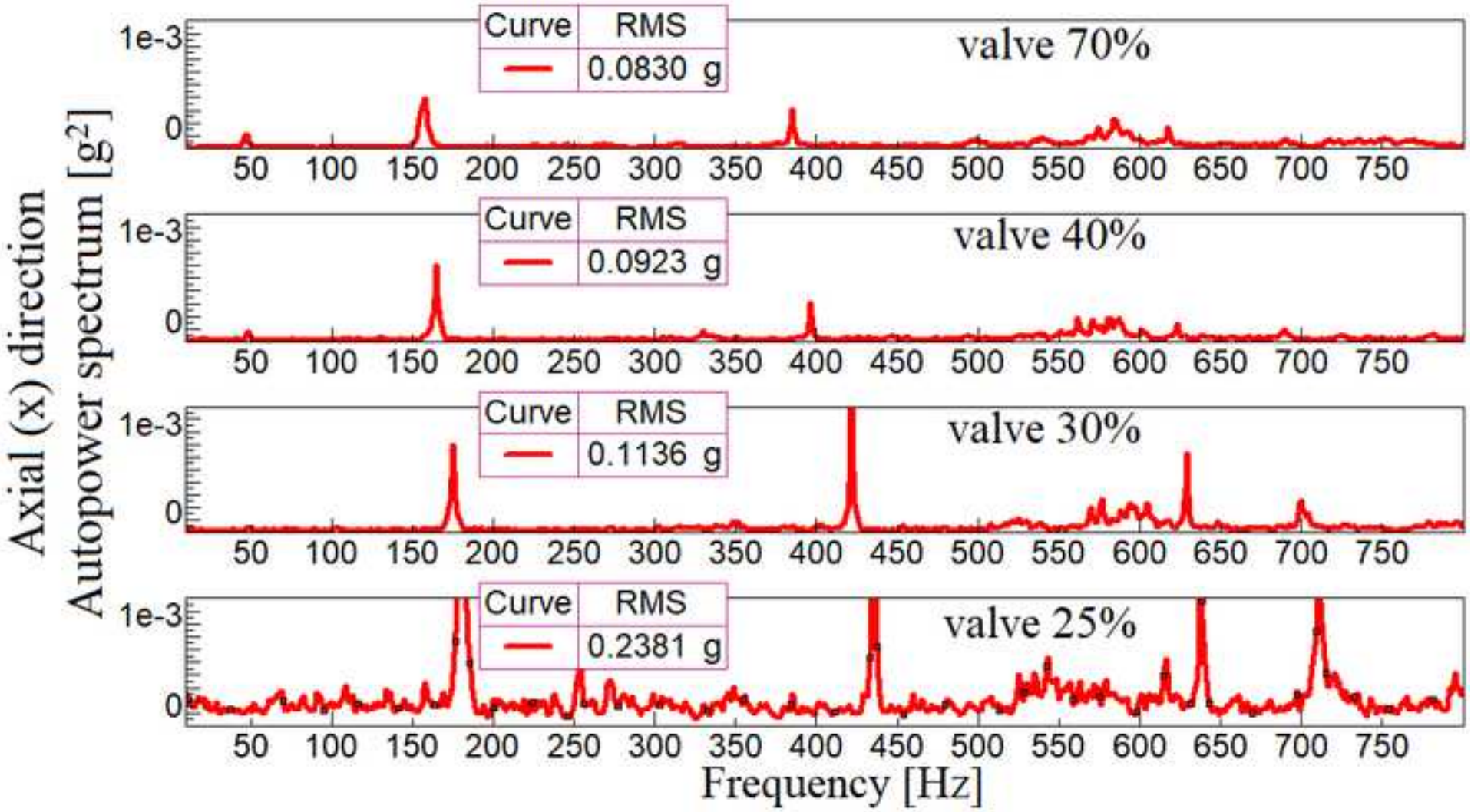

Figure 14

Click here to access/download;Figure;Figure 14.tif

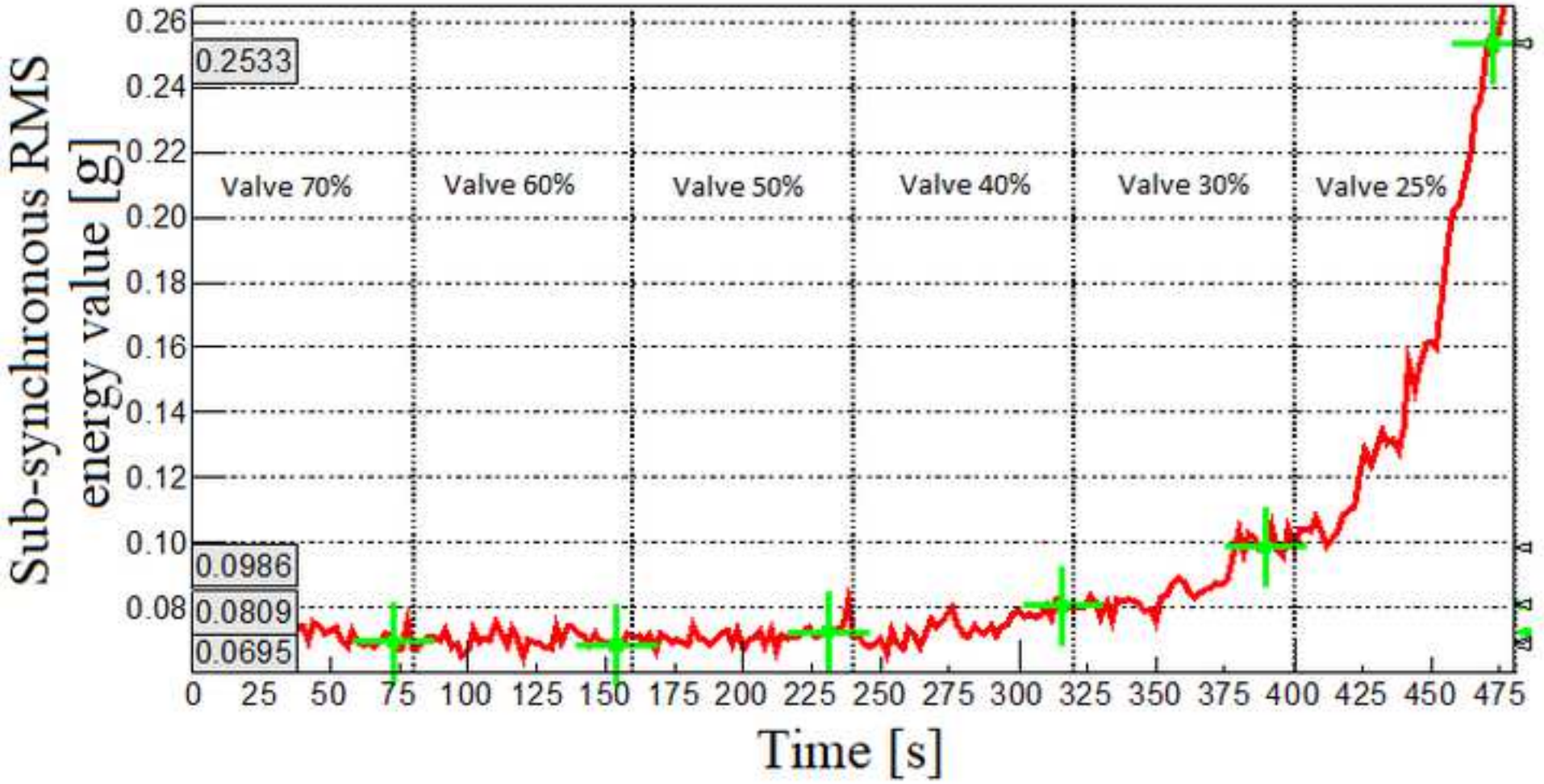

Figure 15

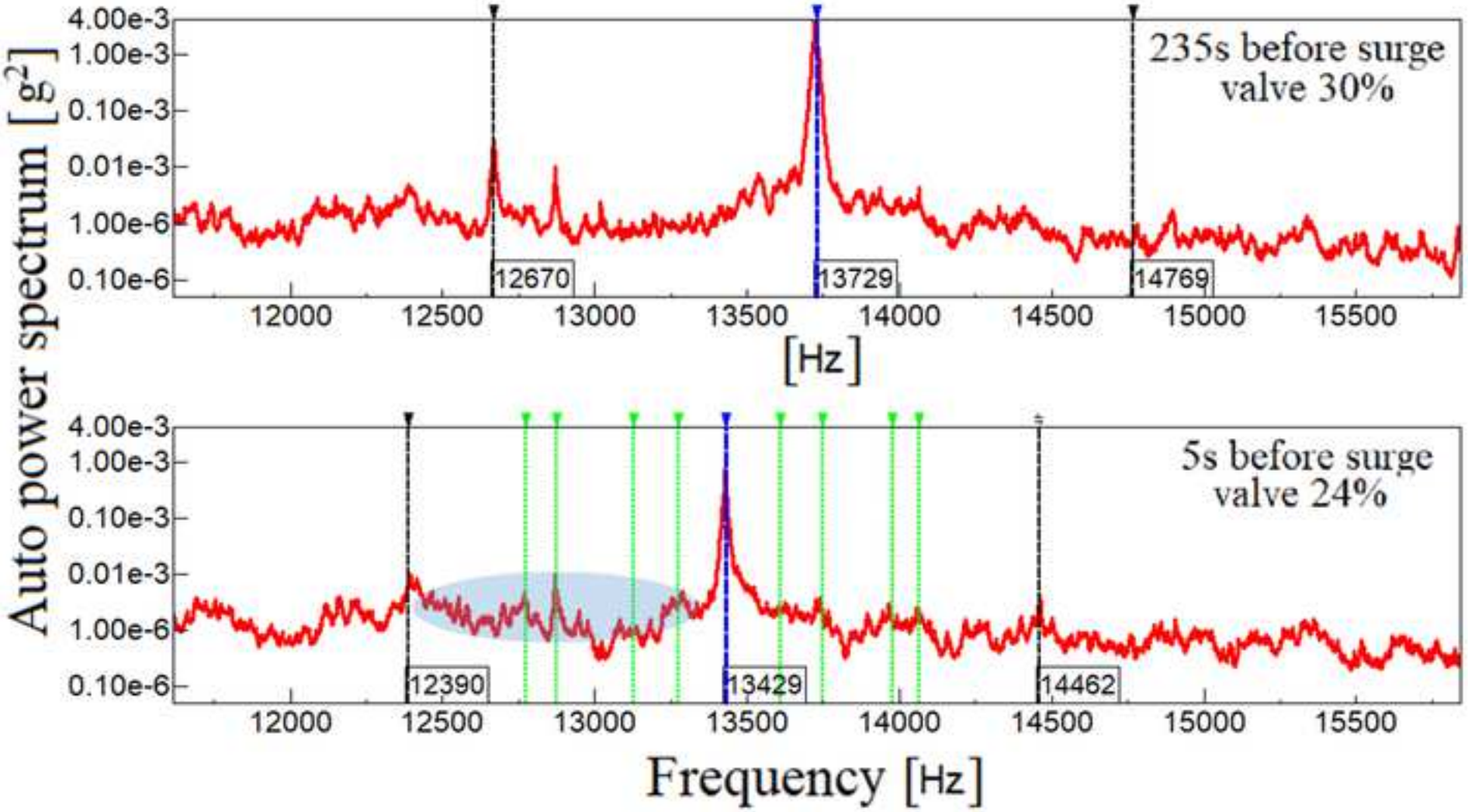

Figure 16

Click here to access/download;Figure;Figure 16.tif

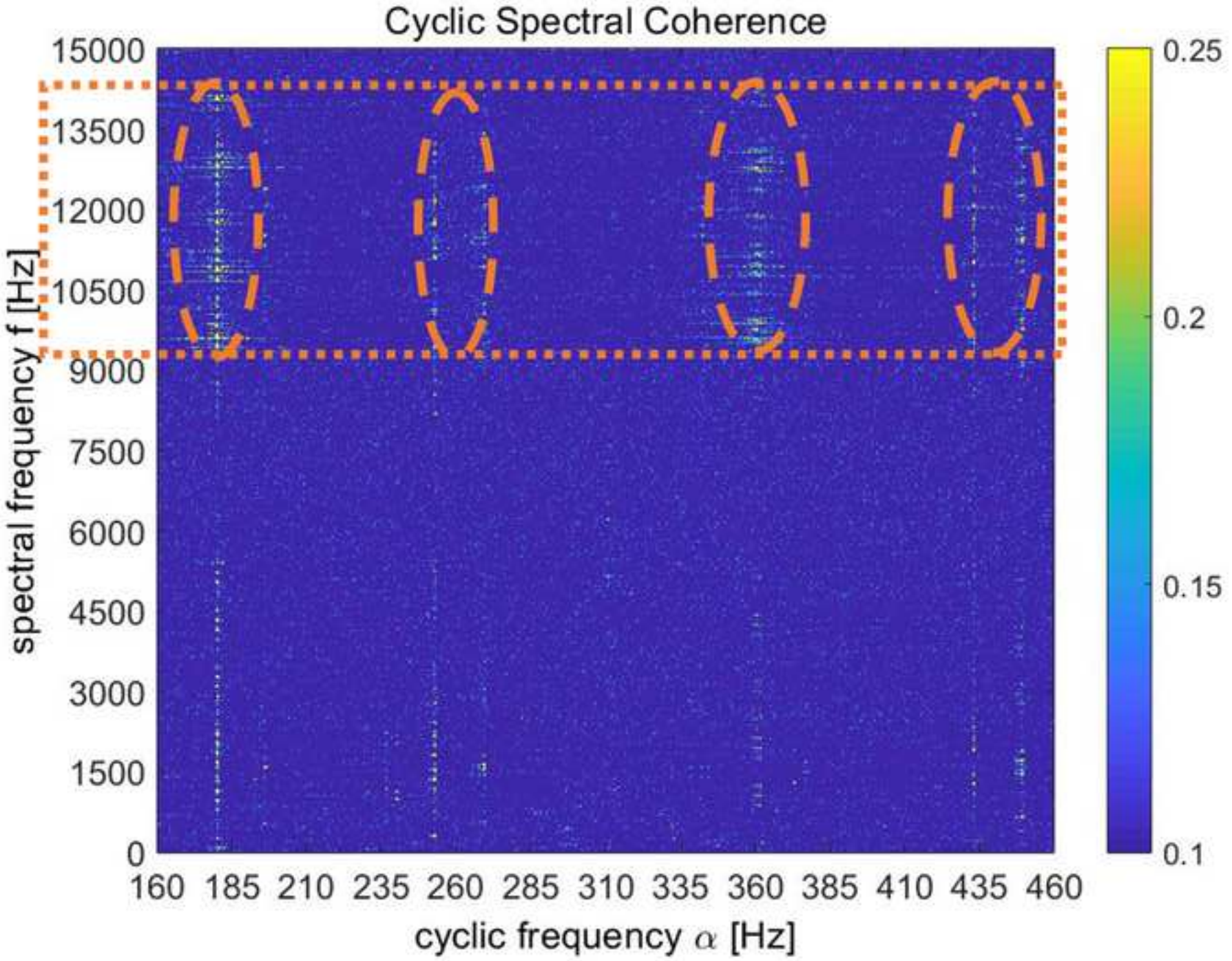

Figure 17

Click here to access/download;Figure;Figure 17.tif

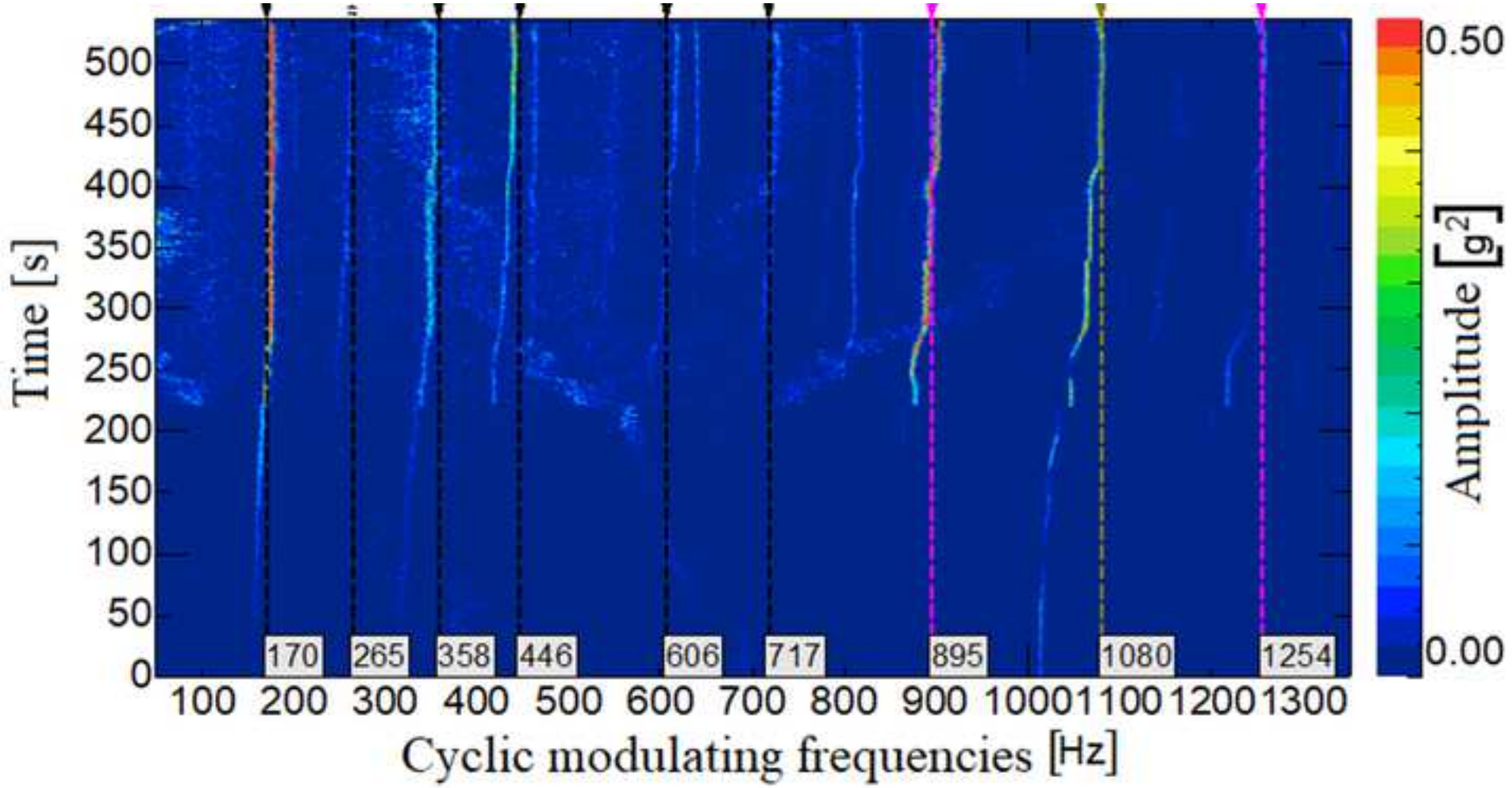

Figure 18

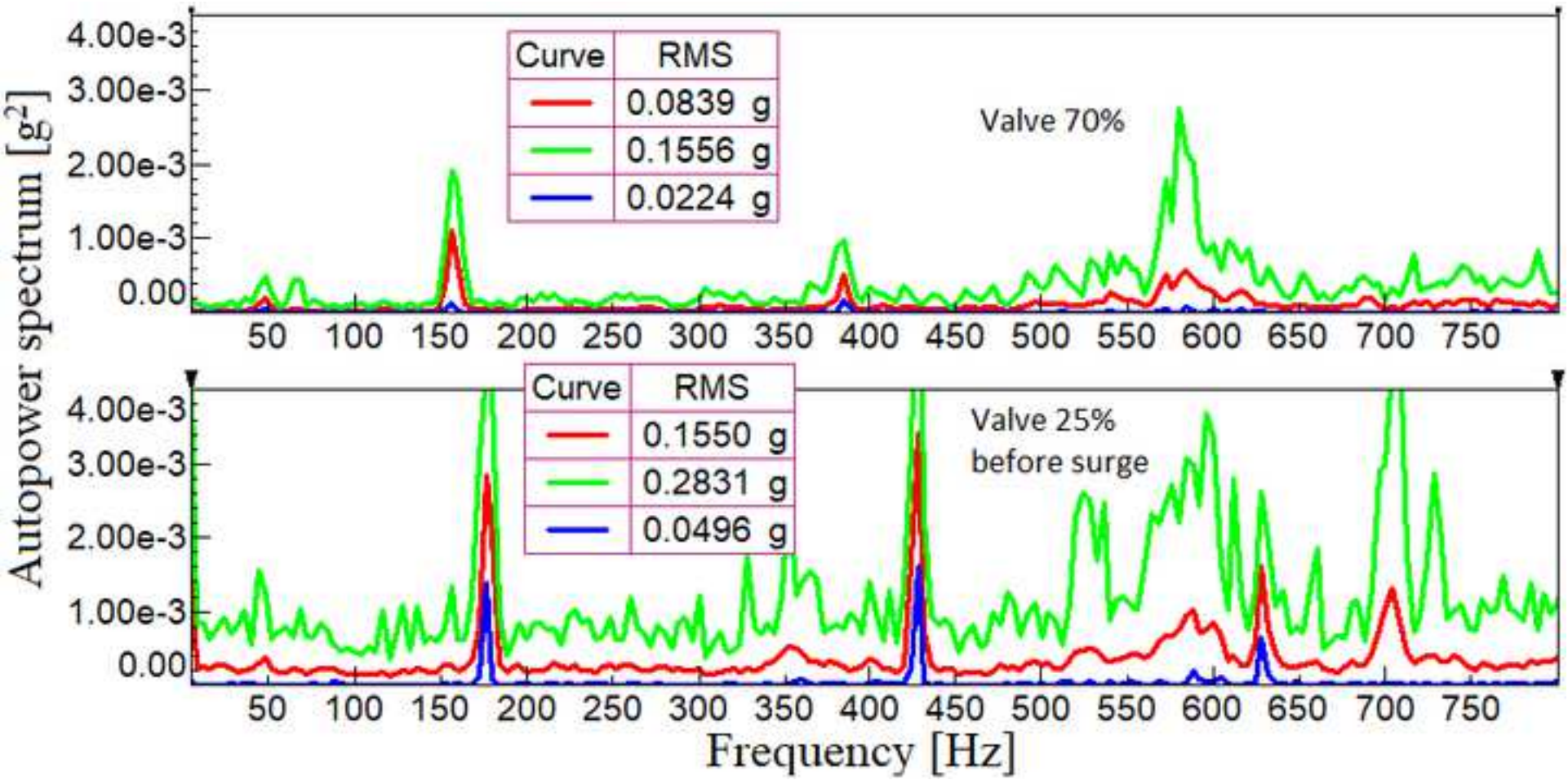

Figure 19

Click here to access/download;Figure;Figure 19.tif

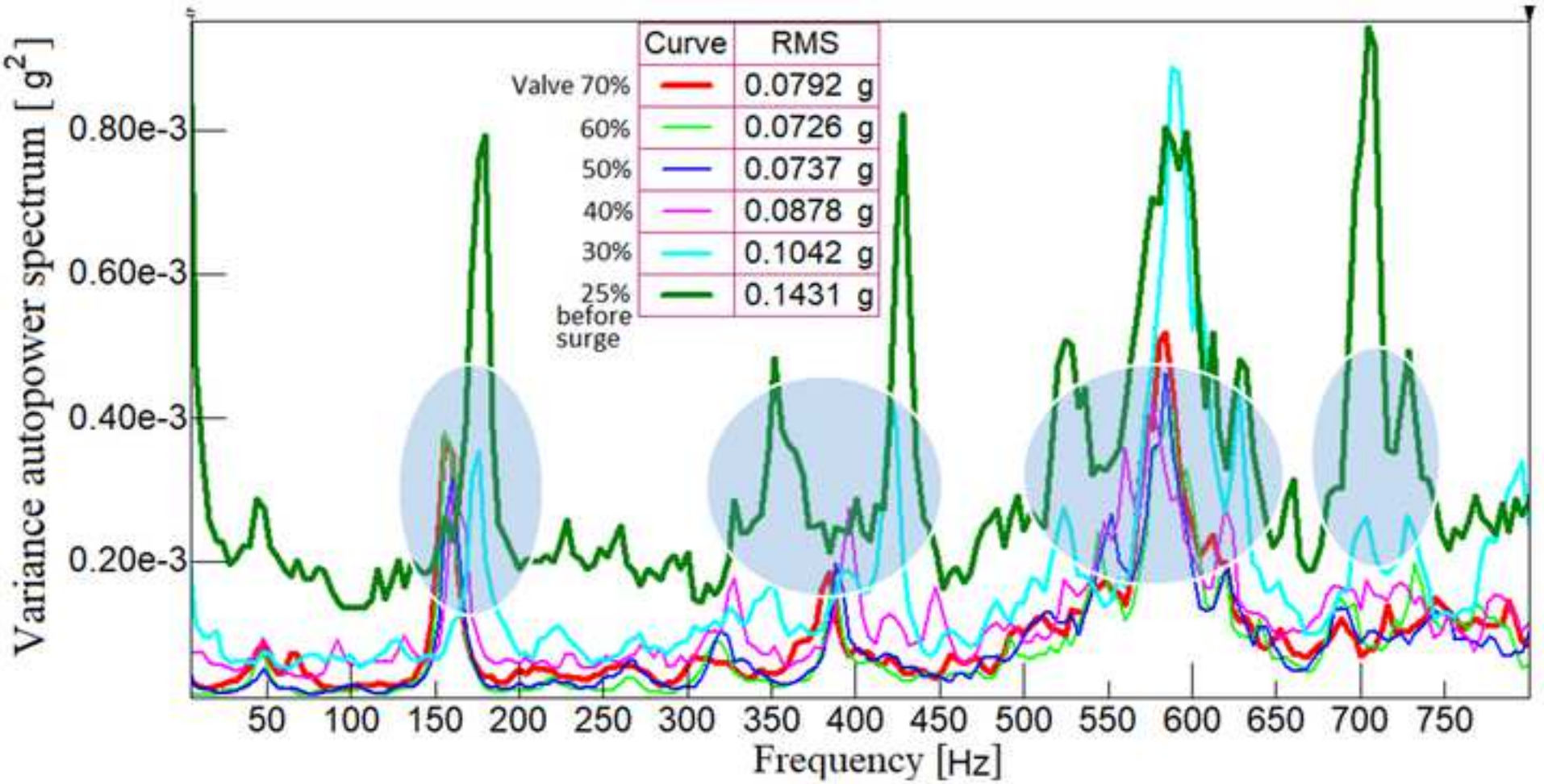

Figure 20

Click here to access/download;Figure;Figure 20.tif

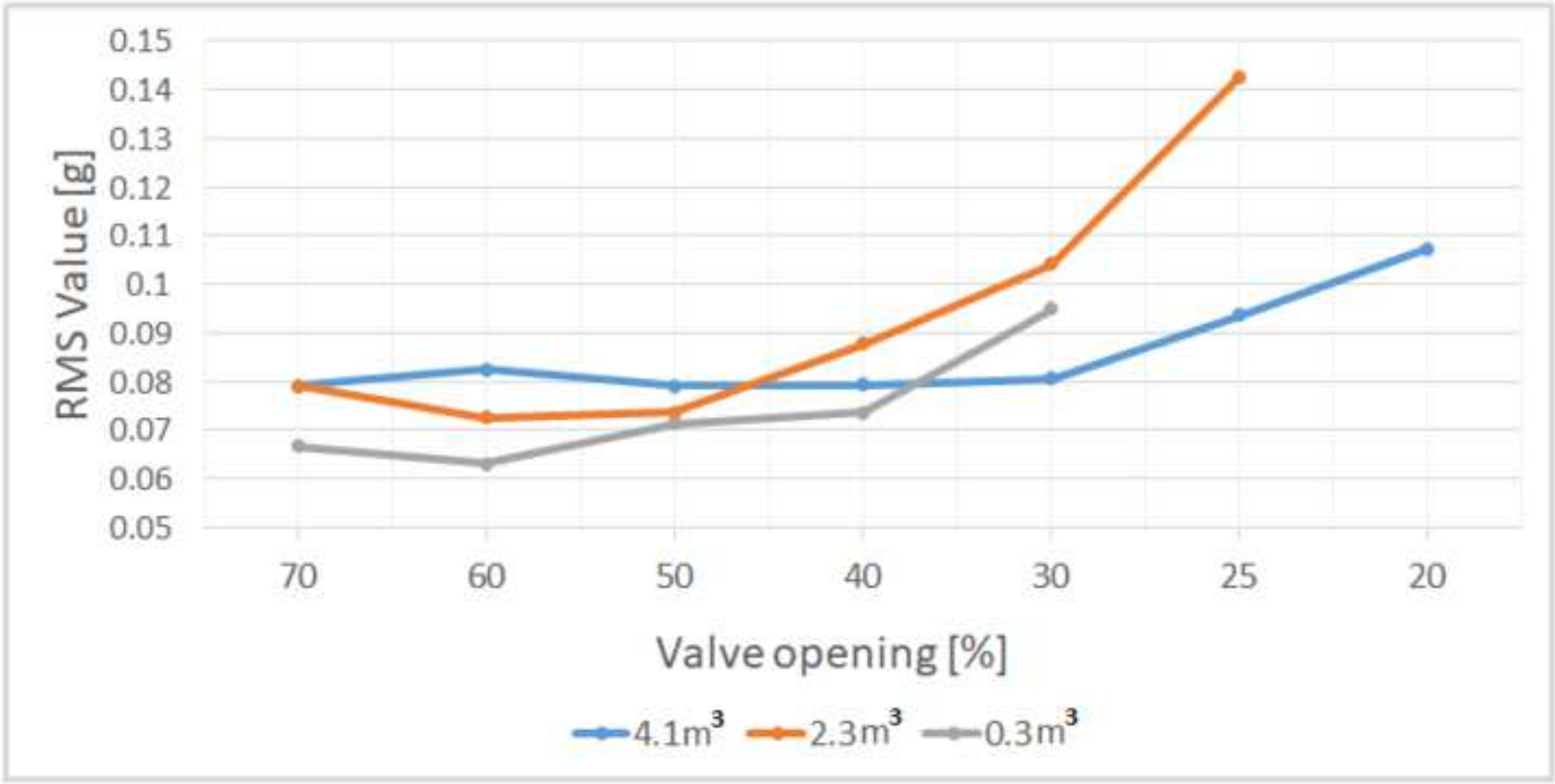

Figure 21

Click here to access/download;Figure;Figure 21.tif

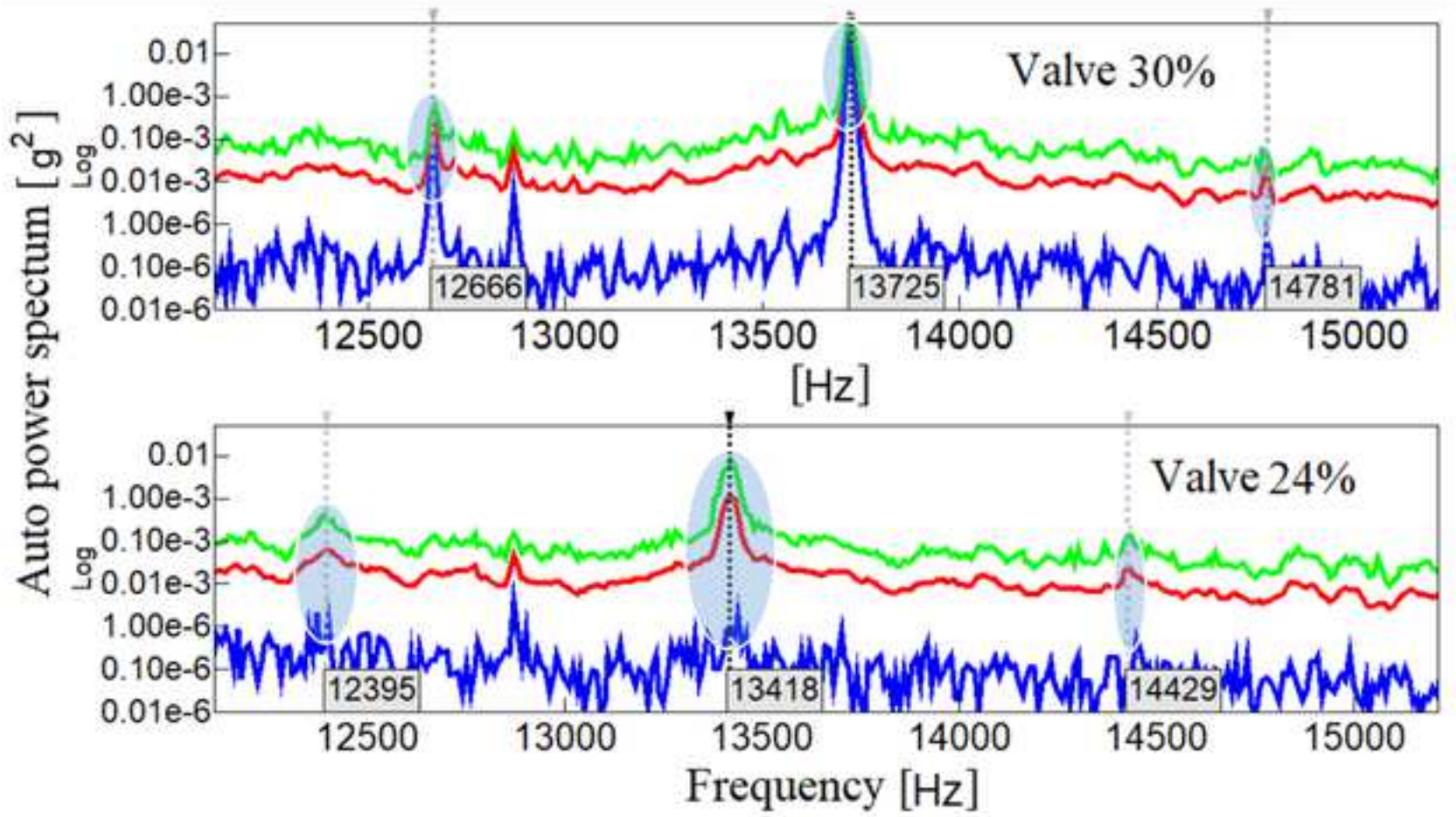

Figure 22

Click here to access/download;Figure;Figure 22.tif

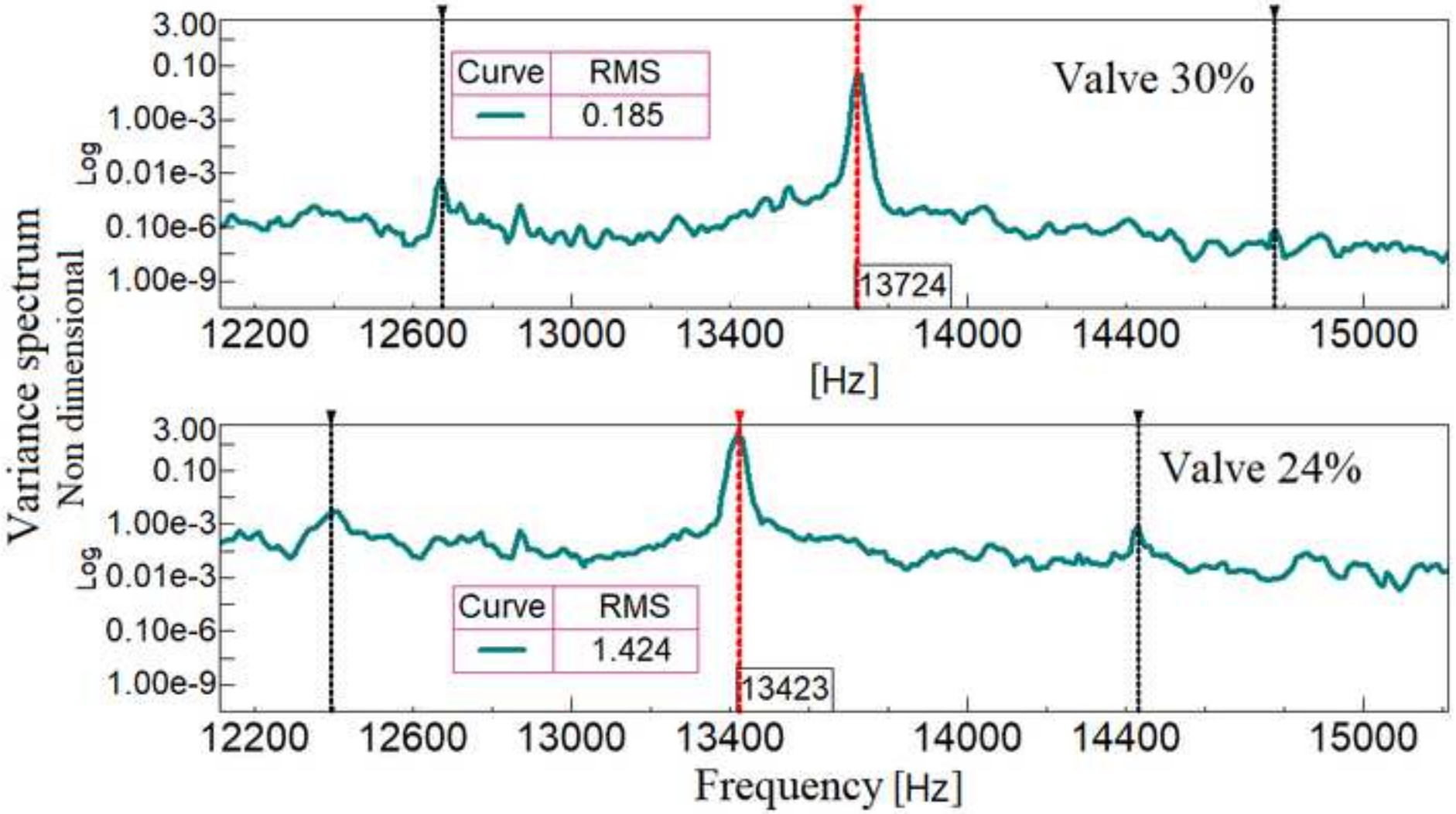

Figure 23

Click here to access/download;Figure;Figure 23.tif

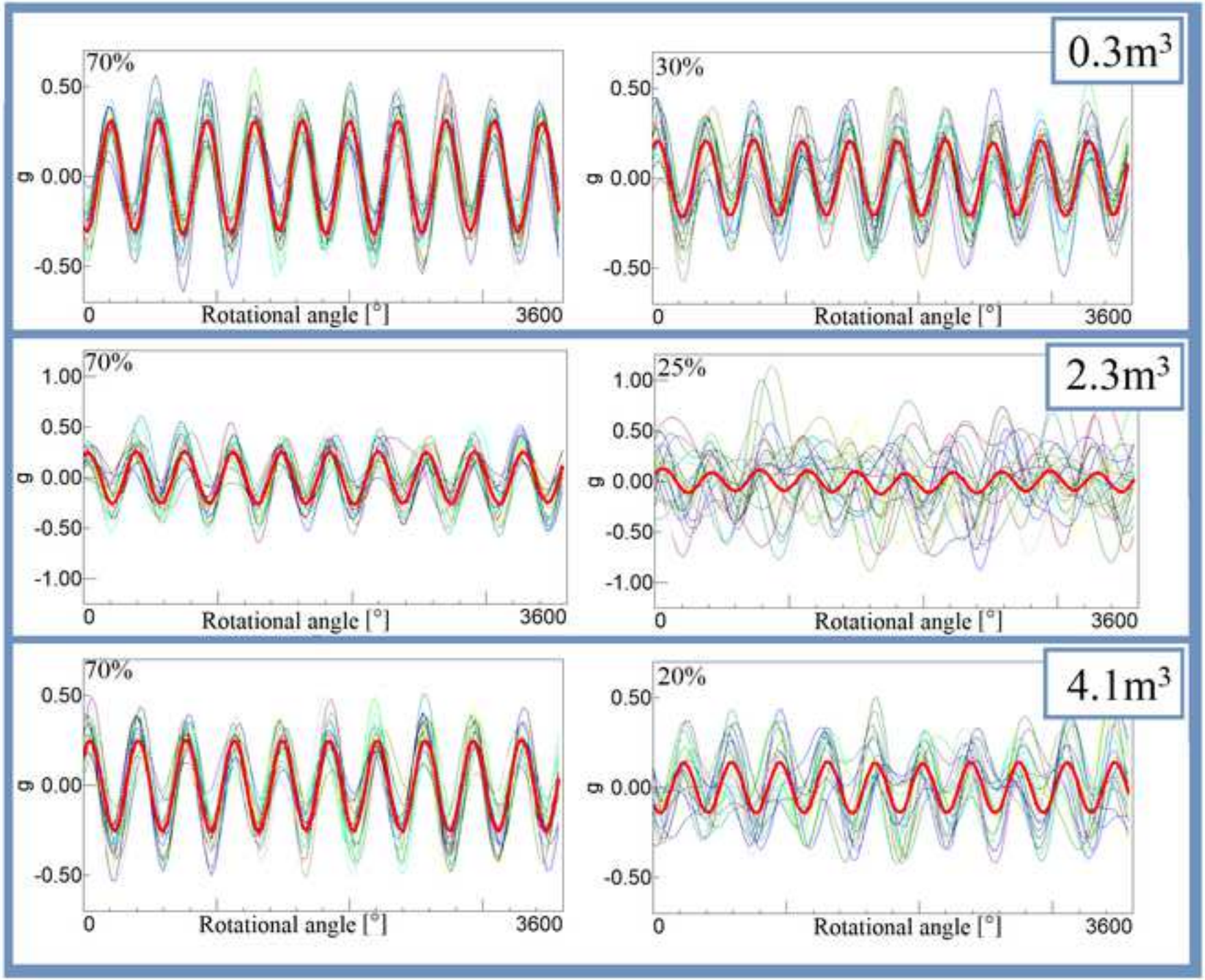

Figure 24

Click here to access/download;Figure;Figure 24.tif

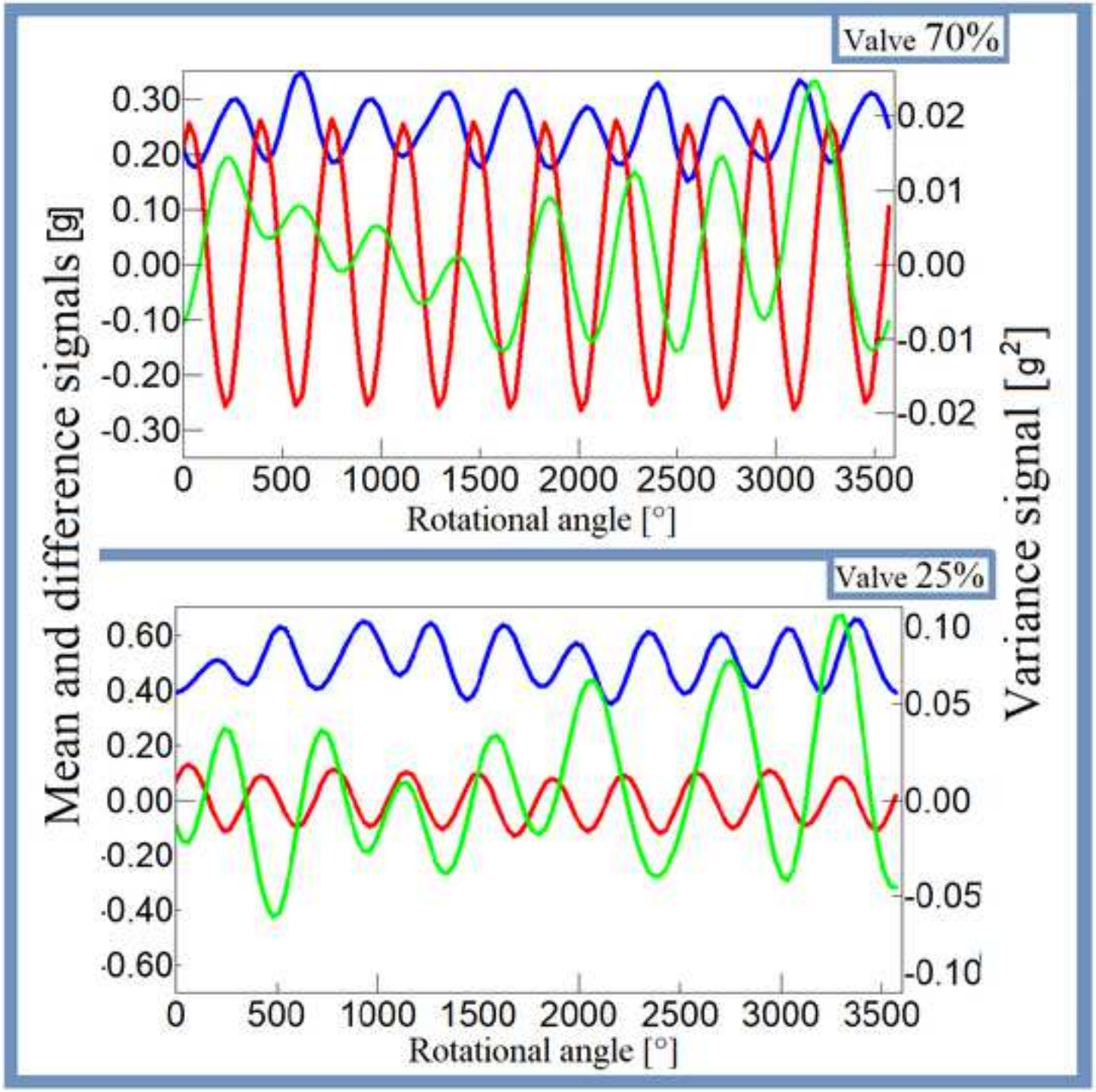

Figure 25

Click here to access/download;Figure;Figure 25.tif

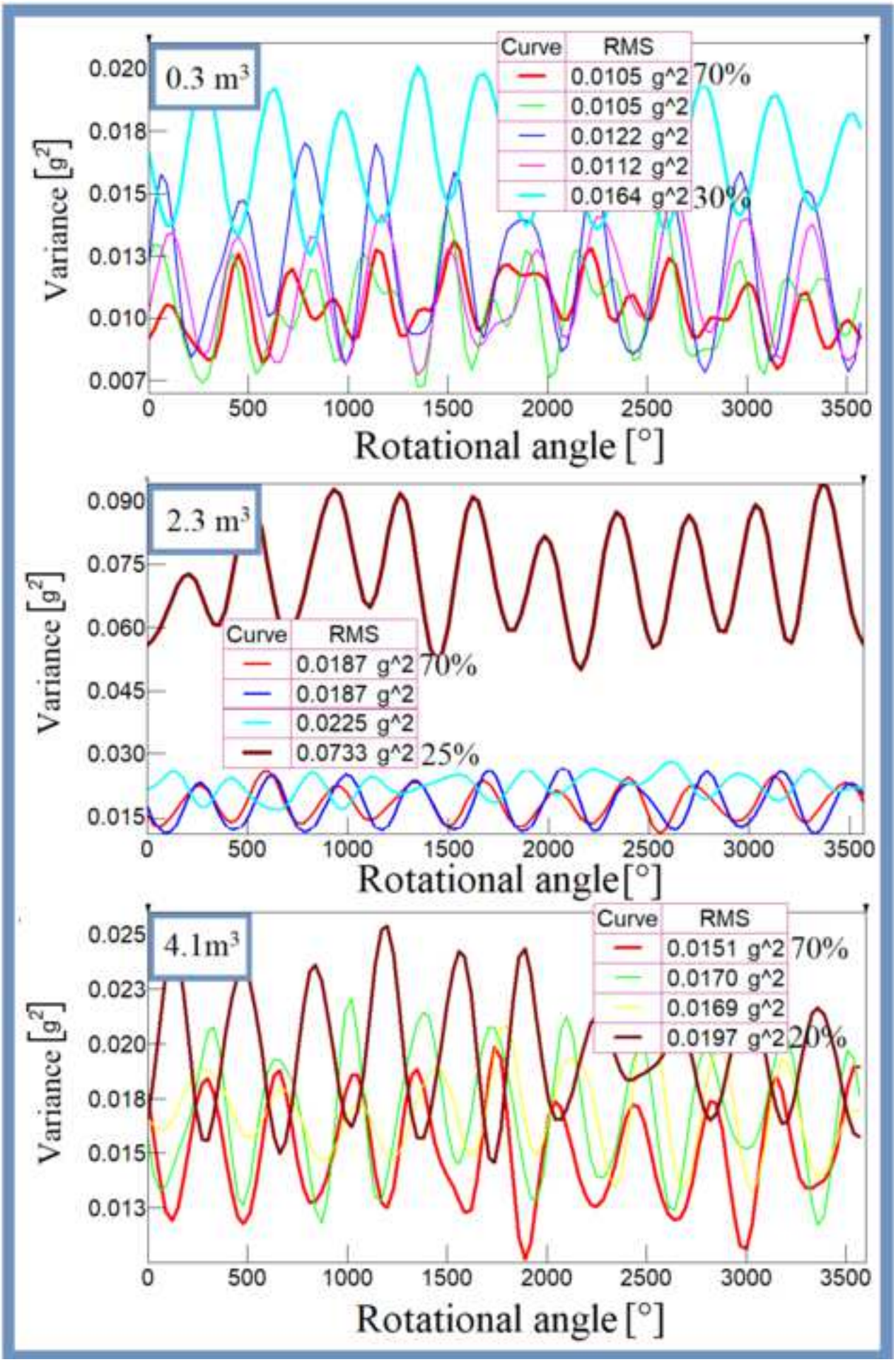

Figure 26

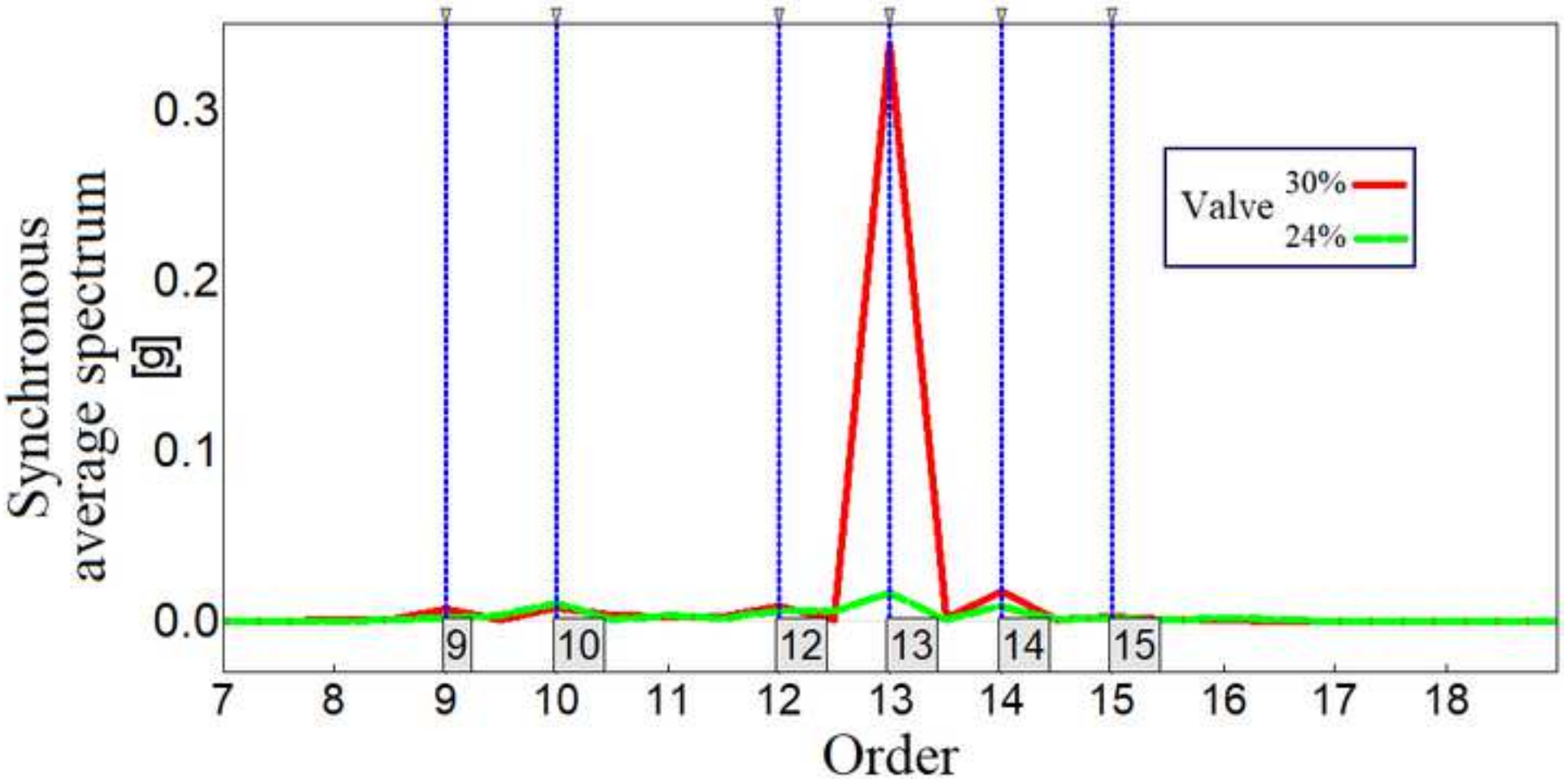

Figure 27

Click here to access/download;Figure;Figure 27.tif

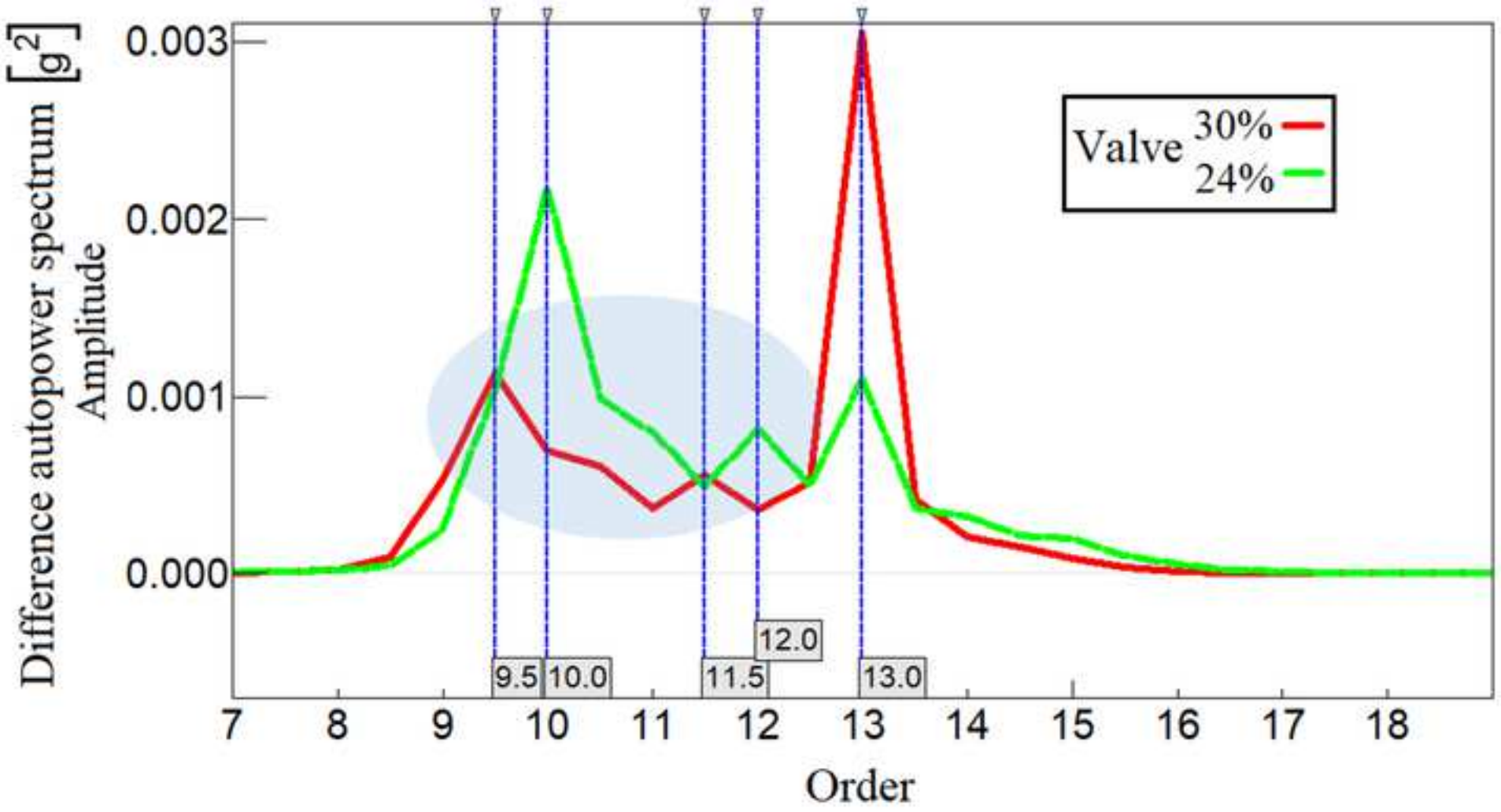

Figure 28

Click here to access/download;Figure;Figure 28.tif

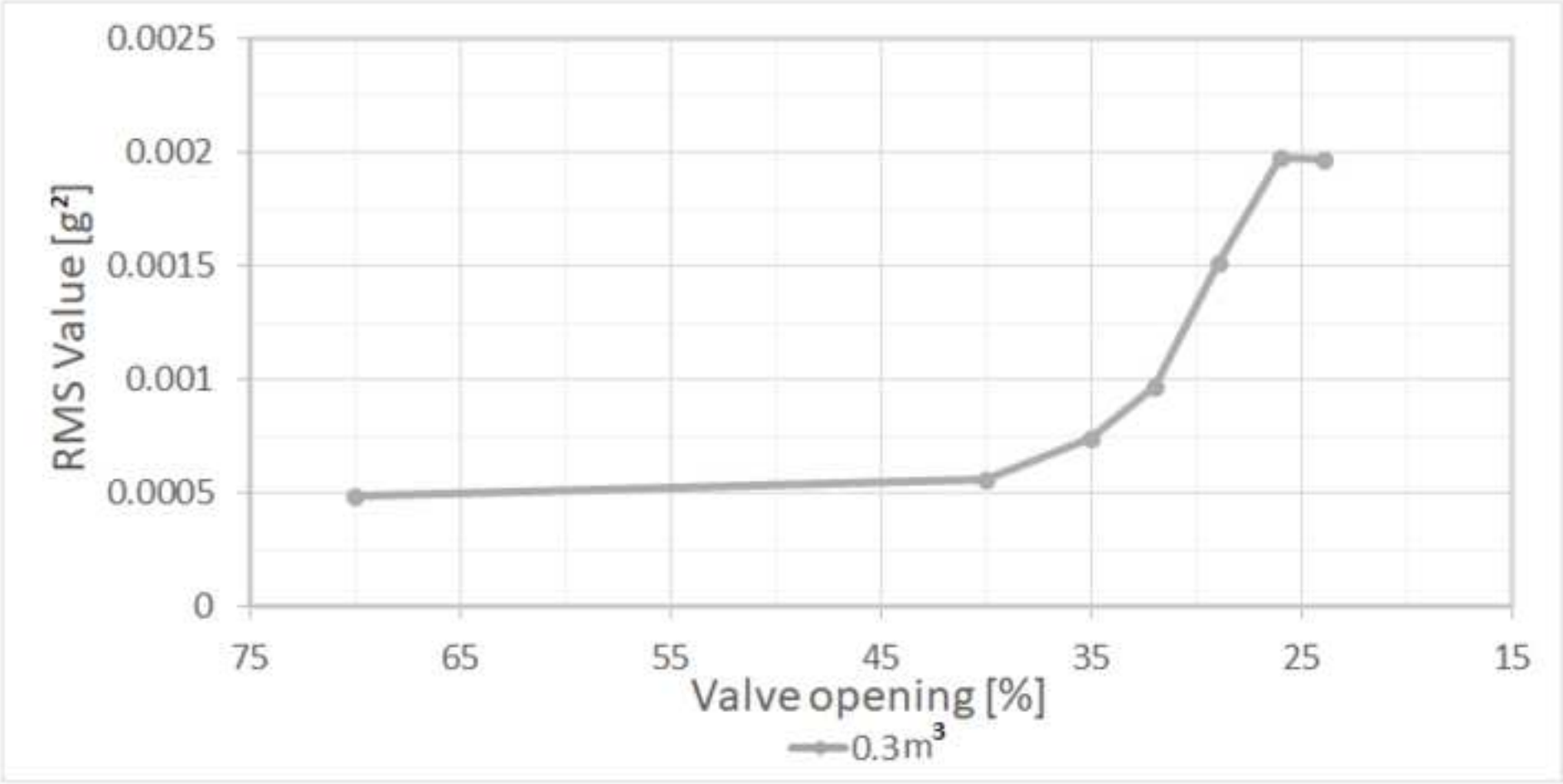

Answers to reviewers

Click here to view linked References